SUBSONIC SPEED ANALYSIS OF BLENDED WING BODY

Submitted by

AYESHA IDREES **FA19-BME-023**

ALISHBA JAVED **FA19-BME-039**

Final Year Design Project Report Bachelor of Science in Mechanical Engineering

Spring Semester 2023

COMSATS UNIVERSITY ISLAMABAD

Wah Campus – Pakistan

Faculty of COMSATS Institute of Information and Technology

COMSATS University Islamabad
Wah Campus
Department of Mechanical Engineering

PROJECT ID	FA2019-FYDP-	**NUMBER OF MEMBERS**	2

TITLE	SUBSONIC SPEED ANALYSIS OF BLENDED WING BODY
SUPERVISOR NAME	**Dr. Muhmmad Shoaib Naseem**

MEMBER NAME	REG. NO.	EMAIL ADDRESS
Ayesha Idrees	FA19-BME-023	fikkzaa@hotmail.com
Alishba Javed	FA19-BME-039	Alishbajaved3129@gmail.com

CHECKLIST:

Number of pages attached with this FYDP report	77
I/We have submitted the complete Project to the Supervisor	✓ **YES / NO**
I/We have enclosed the soft copy of this document along with supporting material in CD.	✓ **YES / NO**
My/Our supervisor has attested the attached document	✓ **YES / NO**
I/We confirm to state that this project is free from any type of plagiarism and misuse of copyrighted material	✓ **YES / NO**

MEMBERS' SIGNATURES

Supervisor's Signature

DECLARATION

"We declare that no portion of this document has been picked from any application or any other university/institute or other institution of learning. This thesis submission is our very own work and to the best of our knowledge".

PLAGIARISM CERTIFICATE

This is to certify that FYDP Title low speed analysis of blended wing body students of Mechanical Engineering Department COMSATS University Islamabad, Wah Campus, declare that their BS thesis is checked by the Department and the similarity index is 13 % that is an acceptable limit as set by HEC.

Name: Ayesha Idrees **Registration No.** FA19-BME-023

Name: Alishba Javed **Registration No.** FA19-BME-039

Date: _____

Supervisor Signature: _____

ACKNOWLEDGMENT

Foremost, all thanks to Allah Almighty for giving us strength, enlightening our knowledge and making us capable enough of completing this project.

Next we would give our warmest thanks to our supervisor Dr. Muhamamd Shaoib Naseem for the continuous support in our Final year project and thesis report. His guidance was always a helping hand towards this project. We could not imagine a better professor for our thesis study. Besides, we would like to thank our co supervisor, Sir Muhammad Awais Hamza for his encouragement and enthusiastic support during all this time. We are grateful to our allied faculty for always being supportive and helping us wherever required.

Lastly, thank you to our family, friends, class fellows for their endless support and believing in us.

CONTENTS

LIST OF FIGURES

LIST OF TABLES

ABSTRACT

With the rising environmental hazards and reduced efficiency in terms of aerodynamic parameters of conventional aircrafts used in commercial flights, a new and modified idea of blended wing body is introduced. Its primary and dominant target is to minimize the consumed fuel during flight operation in order to correspondingly enhance lift values and correspondingly reduce the drag magnitude. Also, the atmospheric emissions are becoming global and worldwide concern as the air vehicles' combustion process discharges certain amount of various gases which comprises of carbon monoxide with addition to nitrogen oxides, generally termed as NOx, which are highly injurious to land and marine life. This project aims to achieve the objectives of getting maximum lift by reducing fuel consumption during flight operation and also find a practical method to optimize the aircraft in such a way that it reduces the carbon imprint from the troposphere. For this purpose, the concept of blended wing aircraft is chosen. First the selection of airfoils was done in order to design such a wing which could fit in the criteria of low speed and low Reynolds number for getting best refined results. A blended wing consists of two aero foils merged together. Hence the aero foils selected were MH78, a reflex aero foil and Selig S1223, an under cambered aero foil which gives maximum lift at low speed. Firstly, the aircraft scaled down model was designed on SOLID WORKS and the process of 3D printing was done afterwards. Next, it was investigated inside the subsonic wind tunnel ESSOM ISO 9001 at low speeds with different angle of attacks including 5°, 10°, 15°, 20° and 25° and at different air velocities to get various aerodynamic parameters. These variables included the coefficient of lift, coefficient of drag, velocity and pitching moment, pressure points and wake regions. After the wind tunnel testing was completed, its computational fluid dynamic analysis were performed on ANSYS WORKBENCH at different angle of attacks and different air velocities for getting the values of same parameters which were considered in wind tunnel experiments. Next, both the results were compared to each other. Subsequently, a full scale model was designed with proper mathematical calculations. This was a radio controlled aircraft whose flight test was performed afterwards via the use of hand-held radio transmitter. This project covers all mathematical design calculation plus the methodology adopted. Its wind tunnel results and ANSYS WORKBENCH results are compared with each other and with free flight testing. Graphical, mathematical and pictorial representation is mentioned in this document.

ACRONYMS

BWB	Blended wing body
MAC	Mean Aerodynamic chord
CL	Coefficient of lift
CG	Centre of gravity
C	Speed of light
SWB	Ship Wing body
AOA	Angle of attack
UAV	Unmanned air vehicle
MTOW	Maximum takeoff weight
CFD	Computational fluid dynamic
MA	Mach number
AR	Aspect ratio
WL	Wing loading
WT	Wind tunnel
PrAdo	Preliminary Aircraft Design and Optimization Program
TetrUSS	Tetrahedral Unstructured Software System

Chapter 1

INTRODUCTION

1.1 HISTORY

The convectional planes were already in use but there was a need of something more efficient which could reduce the carbon imprint and atmospheric emissions from the atmosphere as well as could give a higher magnitude of aerodynamic parameters mainly the value of lift and a smaller drag value and ultimately enhancing the efficiency.

The primary reason of replacing the conventional airplanes with the new idea was due to the emission of carbon oxides with addition to nitrogen oxides which are becoming a global concern for everyone. In order to overcome these issues, the idea of a blended wing body was first introduced by Jack Northrop, who was an American aircraft industrialist and designer, in the year 1940 [1]. Northrop first introduces this flying wing concept when he and his team were manufacturing planes like YB-35 and YB-49 as bombers for military use. Later on NASA was also involved in exploring about blended wings during 1970s and 1980s [1]. Their major focus circulated around finding its effectiveness in terms of noise and fuel reduction. During the year 1990s, Boeing was the one for developing X-36 flying wing. Again NASA made its focus towards flying wings in the year 2000. There has been a major contribution of other industries including European Aerospace industry for finding its advantages for the future aspects.

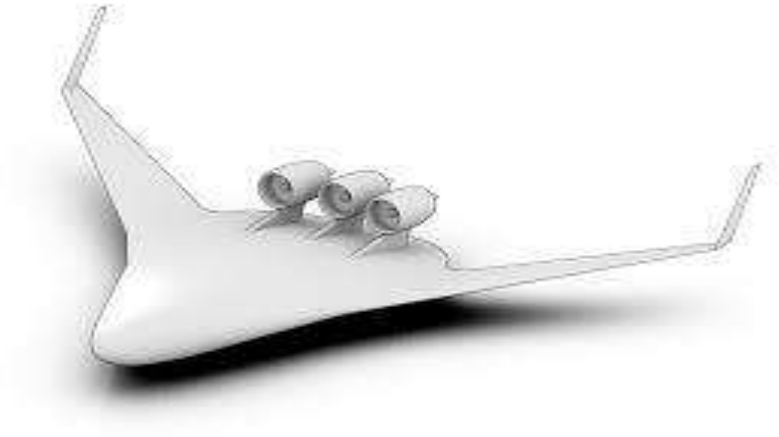

Figure 1: The blended wing body

The blended wing is basically a concept of merging tail surfaces, engines, wings and fuselage all into a single body. The major benefit of this design is that it provides a higher magnitude of lift and correspondingly lower magnitude of drag and at the same time serves as fuel efficient air vehicle plus a great contributor in reducing noise pollution. For making the blended wing stable, an entirely new concept of elevon was introduced which was basically replacing the vertical and horizontal stabilizers and transforming the controlled surfaces into a new feature previously absent in the conventional aircrafts. In the year 1946, the first prototype XB-35 was successfully launched and proved that it was a need of time which was primarily used as bombers during its early release [2].

1.2 TECHNICAL FAULTS AND MODIFICATIONS

By the year 1947, a number of defaults were adding to the failure of this efficient wing design. Specifically in the model of XB-35, several technical problems started to show up. The elevon started to get damaged due to its frequent usage. The test flights started to end early due to the faults such as overheating of the engine, propeller and gear box failures. By the year 1948, another airframe, YB-49 during its flight crashed tragically with the reason of being mishandled while being in high power. Failure after failure eventually rooted to keep the idea of blended wing aside [1].

By the year 1980, again this concept was revised with modifications to the faults found in the previous wing design and YB-49 was modified into a better version. This new flying wing had the exact wing span as of the YB-49 and had the characteristic of being virtually invisible to radar. Its first flight was a long awaited success after a number of failures [2].

Northrop along with his team, released another flying wing called "Northrop Grumman B-2 Spirit" in the year 1987, with its major role of being a stealth bomber, difficult for radar or sonar devices to detect it. Because of being made up of material such as composite carbon graphite, it had properties of absorbing radar beams, eventually absorbing the infrared radiations which could else help in its detection. Also this material improved its aerodynamic flight properties as well as improves and extended its fatigue cycles [3].

The latest blended wing model released is in the year 2017 by Airbus namely "Meveric", model Aircraft for validation and Experimentation of robust Innovative control, is having a wing span of 3.2m, wing area of 2.25 m^2 and a total length of 2 m. It has reduced the fuel consumption up to 20 percent and works by radio-controlling very efficiently [4].

With the advancements in aviation, blended wing is found to be the most efficient aircraft design with maximum advantages which does not only gives better aerodynamic behavior but also is an environmental friendly aircraft structure within the prescribed sustainable development goals. Its higher coefficient of lift and less fuel utilization has made it the finest wing design. This idea is now replacing the conventional plane slowly and gradually [5].

1.3 CHARACTERISTICS OF BLENDED WING BODY

The BWB provides a wide range of advantages in comparison to the conventional planes and this makes its efficiency higher compared to the conventional ones which are tube-and-wing configurations. Blended wing compromises of two aero foils merged together into single body. This means it has no clear distinction between the fuselage and the wings, hence they both blend together in order to make a single surface. It has a short fuselage and no vertical tail rather haves a V type tail [4].

The wetted area and the wing root area is less in magnitude which helps in reducing the surface drag value and offers a large wetted aspect ratio. Its overall standard empty weight is less and evenly distributed throughout upper and the lower surfaces of the craft. The central body carries the lift value approximately equal to 31 to 43%. The fuel efficiency is higher which is almost equal to 10.9% and also the transportation cost is less due to less fuel consumption. A BWB aircraft has decreased longitudinal and directional static stability and damping [5].

The whole surface of the blended wing acts as a lift generator. Its shape is designed in such a way which effectively reduces the drag. The main belly of the craft is broad and vast that helps in accommodating more passengers, cargo and can carry more fuel. Also its shape helps in a better and wider seating pattern for the passenger Due to its unique structure; it needs more careful handling and maintanence of weight distribution [6].

Figure 2: Blended wing body prototype

1.4 OBJECTIVES

This projects aims to validify weather this new idea can be adopted in the future crafts. The objective of this project is to perform research upon the blended wing structure, its manufacturing and its testing to find out its aerodynamic parameters and behaviors and study those parameters which could provide better results and an optimized structure.

Such wing design is a need of time which can offer high value of lift and thus reducing the drag value. Mentioned below are some main postulates which cover our major objectives of the project:

- To perform subsonic speed analysis at different angle of attacks and various air velocities, in order to study the corresponding changes in different aerodynamic parameters.
- Improvement in the aerodynamic parameters by alterations in wing design and finding the best possible wing design.
- Reduction of fuel consumption and combustible gases which are adding to the environmental hazards.
- To study the gliding performance of the BWB aircraft.

- To find the ways of increasing the magnitude of lift and correspondingly decreasing drag magnitude.
- To increase passenger capacity.
- Decreasing the noise pollution and fuel consumption.

1.5 SUSTAINABLE DEVELOPMENT GOALS

One of the most vital objectives of this project is to cover the instructed sustainability goals provided by the united nation in order to promote safe and secure work and green environment. The emission of the hazardous gases to the environment because of the use of conventional planes is damaging not only the atmosphere and the ozone layer but also playing a significant role upon the human and other living organism's health at the same time. Through this research work, a significant role can be played for solving the environmental issues as this projects main goal is reduction of fuel which directly means less exhaust gases to the surrounding [7].

Also this will help in future developments in the field of aviation. Keeping in view the SDG's provided by United Nations, this project is covering the following goals:

- **Goal 3: Good health and well-being:**

  The major concern of the shell and tube planes is the emission of very dangerous gases casing a lot of problems to the nature and human life. Maintenance of good health is very crucial aspect to all living organisms and this new design promises in reducing such harmful emissions.

- **Goal 4: Quality education:**

  Through this informative research work, a good educational wise information and data are is being saved and this will be a helping hand to the future researchers.

- **Goal 8: Decent work and economic growth**

  This project, if carried out in real life scenario, is definitely going to be a remarkable job for the country's economic growth as well as a plus a helping hand to the global climatic issues. This plane, as already mentioned performs a fair job in saving fuel amount, will

help in economic growth and prosperity for any nation and reducing emissions will help us fight climatic changes.

- **Goal 11: Sustainable cities and communities**

  For making the urban development bearable for living and maintaining life, these areas needs full safety measures taken from any natural or artificial adverse conditions which can make living difficult here. A good, pollution free area is a need for a healthy human life as well as to other living organism.

- **Goal 13: Climate action**

  As the global warming plus the pollution found in different layers of atmosphere is creating a lot of worldwide concerns, immediate actions are required to eradicate such issues before it becomes life threatening.

1.6 FUTURE ASPECTS

With the fact of being the efficient aircraft design so far, blended wings are also expected to be the future design of the air travel. Many research works are being carried out in order to find ways of further improving the wing design and flying parameters. Also, focus is to improve lift to drag ratios. Good innovative materials and designing techniques plus the manufacturing ways are in process. Many others ways of improving it to make it more environmental friendly are under consideration [3].

Currently the work being carried out includes usage of high life devices for improving the departure characteristics of the aircraft. The studies are done to enhance the lateral and longitudinal stability. A better location of placement of engines around the plane is being studied which doesn't promote the undesired parameters. The problems related to the structural types are under investigation [4].

It's crucial to remember that creating cutting-edge aircraft designs like the Blended Wing Body requires patience and a large financial commitment. Although the potential advantages of BWB are encouraging, commercial aviation may still be years or even decades away from practical

application. For the sake of influencing the future of aviation, scientists and engineers are investigating novel ideas and technology.

1.7 PROBLEM DEFINATION

The basic problem faced by conventional airplanes is excessive emission of gases. Also a hefty amount of money is required for fuel. Another objective for future aviation is to get such air vehicle which could give better lift magnitude.

In order to fight against the problem of high fuel consumption in the shell-tube structure of conventional planes and ejection of various anti-human gases expelled such a system is required which can help us in achieving the solution of above mentioned problems. This majorly targets green engineering and also covers certain part of sustainable development goals.

CHAPTER 2

LITERATURE REVIEW

By the utilization of conventional aircraft for different motives including air travel, military jobs, transportation, the Earth in being exposed to damaging gaseous mixtures mainly comprising of massive amount of carbon and nitrogen oxides. Also the amount of fuel required is making air vehicles extremely big-budget mode of transportation. For the purpose of improving efficiency and reducing the impact of carbon imprint, massive amount of work and research has been carried on the air vehicles in order to reduce its influence on the environment as well as increasing the efficiency of them. But the major objectives were always cleaning the environment and increasing lift with covering maximum distance. Hence since past 8 decades, work is being carried out for achieving these goals. Some notable researches are mentioned in the following paragraphs:

H. J. Shim studied various aerodynamic force and moment coefficients at different angles of attack and yaw angles in a low speed wind tunnel using a scale down version model of the UVAC-1303 blended wing aircraft with lambda configuration. This model made use of the NACA 64A210 airfoil. This model had a wing span of 700mm, a sweep angle of 47 degrees, a body centerline of 413.4 degrees, a twist angle of 5 degrees, and a planform area of 0.127 m2. The results indicated that yaw had little effect on the lift curve. Maximum lift coefficient was 0.868 at 20 degree angle of attack in the situation of 0 degree yaw angle, and zero lift angle of attack is around 0.75 degree. At angles of attack larger than 10 degrees, the yaw angle influence on drag coefficient is observed. The effect of yaw angle on lift and drag was minimal. Controlling yaw-stability at high angles of attack can also be tricky. Yawing moment coefficients at 10 and 15 degrees of attack showed a very erratic pattern, however at 5 degrees of attack, the yawing moment behaved consistently with yaw angle, leading to 'pitch-break' type behavior. This implies that yaw-stability control may be problematic at high angles of attack. It is easy to discern a tightly linked behavior of rolling moment on yaw angle, as well as a very irregular trend. The pressure distribution curves at 6 and 8 degrees of attack did not reveal any leading edge separation; however at 12 degrees of attack, several flow separation patterns were seen. The

pressure sensitive paint measurement reveals that flow separation begins from the outboard section of the wing, resulting in the pitch-break occurrence [8].

Payam Dehpanah investigated the blended wing model in two stages. First a one percent model was investigated and then based on its results next full scale model was investigated. For the first model, the aero foil Selig S5010 was used. The baseline geometry was obtained by extruding the aero foil Selig S5010. The computational fluid dynamic results showed that during cruise flight conditions, up till 24 degree due to lower aspect ratio and high sweep back angle. Next, maximum span wise lift was obtained in 0.15 m far from the center line. Minimum drag was obtained in a negative. The pitching moment coefficient was negative after $-4\circ$, and also the curve slope was negative before 5^0 and after of 11^0. Therefore, as angle of attack increases, pitching moment coefficient decreases. In between 5^0 and 11^0, pitching moment curve slope was almost zero. The maximum lift-to-drag ratio was obtained in 0.175 lift coefficient. The pressure coefficient remained same, except for slight variation narrowly in the leading edge. In the trailing-edge interconnection between the swept forward body and the swept backward wing, there was a little difference in pressure coefficients between low and high. The second airframe was created by modifying the first. The results were that the wing span was doubled in the second airframe, and the wing reference area increased by 33%. Furthermore, the wing Aspect Ratio was nearly doubled, and the MAC was enhanced by 72%. These little tweaks yielded better outcomes than the previous one [9].

Lixin Wang selected BWB400 aircraft, a BWB with podded engines, to evaluate the flight characteristics. It was then, compared to the B747 BWB. In comparison to the B747, the results showed a wide reference area and a long Mean Aerodynamic Chord of blended wings. Blended wings were discovered to have a relatively low moment of inertia along the pitch axis. The blended wing had highly redundant control surfaces and an array of podded engines. Blended wing aircraft typically used a trailing-edge reflexed airfoil as its central body, which had a huge lift surface and horizontal tail. Due to its short fuselage, the BWB400's aircraft had a comparatively low pitch damping moment. The BWB400 aircraft's Dutch roll mode featured a noticeable oscillation tendency. The directional stability by the V tail was less than those offered by the vertical tail. The yaw axis moment of inertia of BWB aircraft was very substantial. The throttle position was typically fixed through takeoff and cruise flight, the variation in thrust was

relatively minor, and it had minimal impact on the longitudinal motion of the BWB400 aircraft [10].

The optimal aero foil to employ for the wind turbine blades was examined by A. Suresh for low speed wind turbine analysis. The Selig S1223 aero foil was one of them. For S1223, various experiments were carried out, and conclusions were drawn in light of the results. This aero foil was studied with a Reynolds number of 81.72 and various angles of attack that varied from zero degrees to twenty degrees with a two degree increment. It was found that AOA had a significant impact on lift coefficient values. The maximum lift value, 1.77, was attained at an angle of 7°, but as the angle increased, the lift coefficient rapidly declined. At 2°, the highest lift ratio was visible [11].

Rizal E.M. Nasir looked at the efficiency of a blended wing body and found that it was 30% more efficient than a standard airplane. By enhancing lift-to-drag ratio, the BWB idea promised a reduction in fuel consumption of up to 30%. It was discovered that the Baseline-I model was a copy of Lieback's B2 bomber design. The model's wingspan was 0.35 meters, its wing-body plan form area was 0.04 meters square, its mean chord was 0.114 meters long, and its CG was 19.8% behind the leading edge of the mean chord. At a zero angle of attack, the blockage ratio was calculated to be 1.9 percent. In a wind tunnel, this model was studied. All experiments were carried out at an average airspeed of 35 ms^{-1}, a MA of 0.11, an average air density of 1.17 kgm^{-3}, and an average air temperature of 24 °C. These plots showed a linear trend from a -5 to +10 degree angle of attack, with lift coefficient values ranging to -4 to +0.6. However, lift value reduced at an angle of attack greater than +10 degrees. At 0.198c, the gravitational axis was visible [12].

After the blended wing was created, its basic design was being done in 1988 by R.H. Liebeck. There was particular parameter criteria needed for the designing procedure. This procedure was consisting of these further mentioned points. Firstly, the wing's design called for a maximum thickness-to-chord ratio of roughly 17. For the cruising deck angle, it was necessary to use positive aft camber on the center body airfoils. The minimum nose down pitching moment was necessary for the positive static stability. When creating the blended wing aircraft, certain design criteria were taken into account [13].

Aliya Valiyaff spotted a mixed wing model with a departure weight of 10 kg, travel speed was 70 kph, persistence was 1 hour, wing area was 0.843 m^2, length 2.9 m and airfoil MH78 was used as the air foil. Mh78 had a 6 degree approach and an ideal lift coefficient of 0.694. The performance of the MH78 air foil on negative approaches was quite constrained, with a slowdown approach of 12 degrees, as it is cambered with some reflex. In order to achieve a similar presentation shown at successful sites of attacks, the air foil was disrupted at the wing tips in this manner [14].

A blended wing airplane was designed using the best optimum method discovered after extensive research by L.I.Peifeng and colleagues. BWB aerodynamic design approach was developed by combining optimal design and inverse design methods, as well as various aerodynamic tools like low and high fidelity aerodynamic analysis. The core of the design process was determined to be planform optimization. The aerodynamic properties of the aircraft could be directly enhanced by reasonable planform variable matching [15].

Gang Yu looked towards the BWB's design. This particular SWB model had a length of approximately 40.8 m and a wingspan of approximately 63.1 m. In the span wise direction, there were nine control airfoils in SWB. Preloading reflex airfoils were employed on the first four aero foils in the center body to reduce the need for trim, while airfoils four through six were placed in the blending area. Other airfoils were positioned in the outer wing. Reflex airfoils were utilized to reduce loading at the junction, and supercritical airfoils were employed for washout arrangement. The RANS equations were resolved using the finite volume technique. To confirm the viability of the software's result calculation approach, the results of wind tunnel experimentation for the takeoff speed of 0.2 Ma, low speed were compared with the CFD calculation results. A smaller model was used for the testing process, which was done at the NPU NF-3 wind tunnel. Except for the pitching moment coefficient at high angles of attack, the CFD results and wind tunnel test results were in good agreement, demonstrating that the stalling characteristic of SWB was soft. The pitch moment coefficient of the CFD and wind tunnel studies, on the other hand, demonstrated the same growth trend at high angles of attack. The flow separation increased the low-pressure area at the blended area of the wing body and unevenly distributed the pressure at the outer wing's tail as the angle of attack rose. It was also discovered that the SWB's aerodynamic efficiency factor was at its peak at Ma equal to 0.8. This

demonstrated that the SWB performs well in terms of aerodynamics at Ma = 0:8. However, because SWB had a drag divergence Mach number of about 0.83, its aerodynamic performance at Ma = 0:85 was mediocre. Winglets were employed to improve the cruise aerodynamic performance of the SWB. By designing high-lift devices with leading edge Krueger flaps and trailing edge Krueger flaps, it also enhanced the SWB's low-speed takeoff and landing performance [16].

Malcom Brown's primary research interests were in the design technique of blended wing aircraft, namely its directional stability, thorough aircraft performance analysis, lateral stability, high lift estimation, longitudinal control, better fidelity Class mass analysis, and noise production. Results showed that hybrid aircraft have more advantages over traditional ones. The findings of the mass estimations demonstrate that the blended wings operated at a lower empty weight than the conventional wings. The aircraft is more efficient because less fuel is used [17].

Majeed Bisharaa and team designed a BWB with a fuselage that was 5 meters long and 15 meters wide. It was presumed that the material in this case was IM7-8552 carbon-epoxy. A parametric Python program was used to model a novel double shell design concept. The results suggested that the maximal stress was lowered to 36% by changing the distances of frame and ribs, while the modifications in skin layups had little effect (under 2%). The linear buckling analysis's initial eigenvalue was raised from 0.82 to 1.26. According to the results of the sensitivity analysis for the span-rib laminate thickness, going from 2 mm to 5 mm thick reduced the maximum stress by 19% [18].

For long-range business jet aircraft, the BWB concept was used to determine whether it was practical or not. It made use of a reflexed (s-shaped) airfoil. Different mathematical formulas were used to design it in order to achieve the best outcomes for business use. The current BWB business jet used three scaled-down Sam 146 engines. It may be concluded that composite materials were preferable to metal materials for the current BWB layout. For this plane, its vertical tail was 378 kg, Wing weight 8371 kg, Fuselage 4429 kg, and Engine (propulsion) 5939 kg. The weight of the crew, fuel, and payload together yield a total aircraft weight of 45800 kg. Most of the forward and aft CG was on 15% and 17% MAC, respectively. Here, NACA 63a2103 was changed to a reflexed camber airfoil. As a result of this design, BWB configuration offered less thrust loading and superior aerodynamic efficiency compared to conventional. Additionally,

good aerodynamic efficiency reduced drag and boosts fuel efficiency. It gave the fuel tank more room. To solve the issues of making the craft stable, there was a solution suggested which tells to consider a reflexed shape aero foil. Also, another effective method is to use winglets which would also help in taking the role of vertical tail and improving aerodynamic performance [19].

By carrying out a number of experimentation on shape and planform, scientists looked at the impact of the design factors and restrictions, the scientist studied the design trade-offs. They investigated how the CG location, needed static margin, and trim limitation affect the BWB optimum shape. They studied the design space further by incorporating wing planform design variables in the algorithm and applying a center plane bending moment restriction. Planform variables were added, which decreased drag even further [20].

The aircraft's specifications in the Kai Lehmkuehler article were 16 kg MTOW, 3 m span, and 15 ms^{-1} stall speed. The wing sweep of this aircraft was kept to a maximum of 15 degrees (for roll stability) in order to prevent the tip stall tendencies that higher sweep at high lift coefficients can cause. The 10% thick S5010 aero foil was used as the wing section. The aero foil was changed in X-Foil into an S5016 with a 16% thickness to provide the necessary volume for the body section. Other features of this aircraft included a single large elevator that took up 20% of the main body chord, twin fins on either side of the elevator, wing tips that were canted upward to add additional dihedral, tricycle landing gear, and a final wing area of 1.53 m^2 with a body length of 1.25 m. According to the mean aerodynamic chord, all statistics were presented at 20 ms^{-1} tunnel speed for wind tunnels, which corresponds to a Reynolds number of 450,000. Lift is a 4.15 / rad experiment. According to wind tunnel results, the maximum lift coefficient raised with airspeed, reaching 0.96 from 0.93 at 13 ms^{-1}. The flight's center of gravity was at 0.6m. The flight testing demonstrated good handling qualities in flight and the wind tunnel tests nicely matched the projected data [21].

The wide oval cabin, a novel idea for a pressure cabin design for blended-wing-body aircraft, was introduced in this study by Francois Geuscan. It is thought that the broad oval cabin could replace non-circular pressurized cabin types which were already in use. The cabin design had a perimeter created by four arcs of various radii that join smoothly, enabling a flexible cabin arrangement and a fusion of structural and aerodynamic design. The oval cabin design for the blended wing body uses arcs of varying radii of curvature to carry pressurization loads and an

internal box structure for compression and tension stresses, resulting in a structurally efficient and capacious cabin. The design enabled for modification of cargo storage and passenger accommodation, and is well-received by customers because to its versatile cabin arrangement. Enhancing weight calculation methods, researching the connection between the main cabin and the outer wing, and assessing the aircraft's overall performance were the key goals of further study [22].

The Blended Wing Body (BWB) business jet was a new concept that aims to solve the fuel efficiency problem of long-range aircraft. The design of the BWB business jet focused on high subsonic speed, high aerodynamic efficiency, and stability and control solutions. The BWB configuration allows for nonstop flights over long distances, provides more space for passengers and fuel, and reduces drag for increased fuel efficiency. The use of reflexed camber airfoil, winglet, and control surfaces on the wing helps to address stability and control issues [23].

BWB UAV Green Raven developed by KTH in Sweden analyzing the flight characteristics, aiming to improve fuel efficiency and payload capacity. The analysis in ANSYS Fluent 2020 R2 include extrapolating lift, drag, and pitching moment coefficients, evaluating aerodynamic efficiency and stall patterns. To properly analyze the Green Raven, a more powerful computer with more RAM memory was needed to run simulations in ANSYS Fluent and conduct domain independence and mesh convergence studies [24].

The structural analysis of BWB aircraft configurations was conducted using a multidisciplinary process called PrADO. PrADO enables the creation of detailed finite element models and loads for different flight conditions, allowing for iterative structural sizing and mass estimation. The process included an overall aircraft optimization loop that considers fuel consumption, aircraft mass, and operating costs, leading to configuration improvements and integration of different structural solutions. The evaluation capabilities of the preliminary design program PrADO for BWB aircraft had been improved by incorporating physics-based mass prediction and real geometry considerations. The methodology for weight prediction and design-specific details in pre-design had been demonstrated, which could be valuable for future weight prediction and structural design optimization in preliminary aircraft design. The research assessed the feasibility and efficiency of a large blended wind body aircraft, finding a 20 percent increase in transport productivity without new safety or operational issues [25].

The research assessed the feasibility and efficiency of a large blended-wing-body aircraft, finding a 20% increase in transport productivity without new safety or operational issues. It was observed that the consumption saving of the BWB model represented a 25% with respect to the conventional airplane. Winglets and other design devices were being investigated to improve the values of the airplane. The study suggests that a fly-by-wire control system may be necessary due to the negative static margin in relation to engine location. The future of this airplane depends on factors such as cabin size, passenger comfort, and evacuation strategies [26].

The BWB concept involves carrying the payload within the inner wing of the aircraft, which requires deepening the aero foil sections. Design and mass prediction challenges arise when pressurizing the non-circular cross sections of the blended wing region. A method has been developed to predict the airframe mass of BWB designs, although it lacks full validation due to the absence of actual aircraft [27].

Rong Ma proposed a hierarchical multi-objective optimization approach using the S1223 airfoil to design a high-performance propeller for low-dynamic aircraft in Near Space, resulting in an optimized airfoil that meets the design requirements for low-dynamic vehicles in the stratosphere. According to the S1223 airfoil results, the improved S1223_OPT2 airfoils, which was based on the S1223 airfoil's high lift and low Reynolds number, satisfied the optimization design specifications and exhibit excellent aerodynamic properties under both design and off-design conditions. The hierarchical multi-objective optimization platform and the multi-optimized airfoil can be utilized as references when designing high-efficiency propellers for low-dynamic vehicles in the stratosphere [28].

Rong Ma investigated about the aerodynamic characteristics of airfoils in the low Reynolds number condition, specifically for the application of propellers in low-dynamic aircrafts in Near Space for finding the most optimized aero foil shape to be considered. The aerodynamic performance of airfoils in this application was mainly affected by various parameters like Reynolds number, different angle of attack, airfoil chord length, and another important parameter of airfoil relative thickness. The numerical simulations of airfoil S1223 using FLUENT computational software and the Spalart-Allmaras turbulence model was used to extensively study and understand various features of aerodynamic performance of low-Reynolds-number and high-lift airfoils. The numerical simulation results were then compared with experimental data,

confirming the reasonability of the simulation for airfoil S1223. The aerodynamic parameters of airfoil S1223 are greatly influenced by relative thickness and Reynolds number, with the best performance observed in airfoil S1223 with relative thicknesses of 12.13% and 5%, suggesting their use for blade root and blade tip respectively, and further optimization research is recommended [29].

Due to its effective aerodynamic design, the blended wing body idea delivered superior performance versus traditional aircraft. The objective of Mark Voskuijl was to create a tool for creating a blended wing body aircraft's flight mechanics model for use in determining its controllability and creating control surfaces. The automated generation of a flight mechanics model for a blended wing body aircraft and other fixed wing aircraft shapes had been made possible using a tool. Uses for this tool included control surface design, handling characteristics analysis, control allocation system design, failure state analysis, and creation of flight control laws [30].

Low Reynolds number airfoil analysis is important for urban air mobility vehicles and unmanned aerial vehicles. The Green Raven project at KTH Aero used reflex airfoils and various models to simulate lift, drag, and moments for MH61 and MH104 airfoils. XFOIL and CFD turbulence models were used. XFOIL provided adequate results for initial design stages, while the turbulence model produced accurate results in a reasonable time. The two airfoils had similar characteristics at low angles of attack, but MH104 was superior near stall. The comparison between two airfoils in terms of their lift and drag performance were observed [31].

However, the MH104 airfoil had clear advantages in terms of producing greater lift and less drag near stall conditions. This meant that the MH104 airfoil was better suited for flight conditions where the aircraft is close to stalling, which is a critical phase of flight. On the other hand, the MH61 airfoil had a more accurate representation of the complications in the shape of the curve, which meant that the theoretical calculations and simulation results were in agreement [32].

Reynolds number, flow type, and airfoil shape are a few examples of variables that affect how well airfoils operate aerodynamically. Scientist focused on the relationship between airfoil shape and the aerodynamic performance of airfoils at low Reynolds numbers. Numerous airfoil geometry characteristics, such as maximum thickness, maximum camber, their placement, and

reflex angle, were investigated. The findings demonstrate that the lift, drag, and moment coefficients are significantly affected by changing airfoil shape and rising Reynolds number [33].

UAV systems are becoming important for precision agriculture and infrastructure upkeep, including dam and road repair. The article gave a general introduction of UAV systems and how they may be used to photograph and document cultural treasures. The first photogrammetric flight over an old community in Peru was conducted using a tiny UAV system that was outfitted with a GPS/INS-sensor and stabilizer, demonstrating benefits over conventional approaches. Image overlapping issues were eliminated by the UAV-helicopter's steadiness in the air, although more powerful engines and accurate GPS/INS systems are required for improved outcomes [34].

Unmanned aerial vehicles (UAVs) are being employed for both military and civilian reasons in aerospace engineering; however their design presents difficulties owing to their intricate configurations and tasks. Traditional deterministic optimization approaches work well for a limited range of issues, but strong numerical tools like evolutionary algorithms (EAs) are needed for multi-modal issues or applications that span several domains [35].

A Blended-Wing-Body tri-jet arrangement underwent low-speed wind tunnel experiments to assess its stability and control capabilities. Simulation investigations on probable uncontrollable flying characteristics will be conducted using the acquired data. A large database for flight simulation and ground-to-flight correlation was produced through experiments on a Boeing-exclusive BWB configuration. The existence of persistent spin and tumble modes with particular controls, restricted directional control authority, considerable control interference effects, and significant impacts of wind tunnel construction on pitching moment were some areas of fault and investigations are being carried to make it more productive. Based on these testing and studies, no significant flaws or restrictions have been found in the BWB flight dynamics [36].

The Blended-Wing-Body aviation design had the potential to revolutionize the effectiveness of big airplane subsonic transport. The BWB was judged to be superior in all important ways in a NASA-sponsored research that compared an 800 passenger BWB airliner with a conventional layout airplane for a 7000 nautical mile design range. Lower fuel burn, takeoff weight, operational empty weight, overall thrust, and a greater lift/drag ratio are all benefits of the BWB layout, as are its large wingspan, buried engines, and relaxed static stability. The BWB idea is a

brand-new technology in and of itself. Neither new materials nor certain old technologies are needed. However, to overcome the difficulties found in the technological disciplines, innovative solutions will be required [37].

The BWB concept is a relatively new concept of an aircraft that integrates the wings and fuselage into one structure, reducing drag and increasing lift. The aim of the research was to design a radio-controlled small-scale BWB aircraft for long-range payload delivery at low altitudes. Four airfoils, HS522, LA2573A, NACA 25111, and MH78, were analyzed in XFLR5, and NACA 25111 and MH78 were selected for the center body and wing, respectively, based on their lift and moment characteristics. The stall speed and wing loading were primary factors in determining the size and area of the aircraft, which resulted in a design with a five feet wingspan. The CG was placed ahead of the aerodynamic center to provide static and dynamic stability in pitch. Twist, dihedral, and sweep were incorporated to increase stability and controllability. The final design was tested for stability using XFLR5 and compared to wind tunnel tests of a scaled-down prototype. The results showed that the 3D Panel Method in XFLR5 closely matched the wind tunnel results, while the computational fluid dynamics (CFD) results did not conform after a 10° angle of attack. Therefore, CFD was deemed unnecessary for designing a plane of this size. A larger test prototype made of polystyrene foam successfully achieved flight [38].

The paper focused on the analysis and design optimization of aero foil profiles for airplane wing design. The authors used CFD to optimize the aero foil shapes and evaluate their aerodynamic characteristics. The research aimed to find the best aero foil profile for use in compressors, turbines, etc., with reduced flutter and maximum life. The results were evaluated within a low-speed subsonic range, specifically for Mach numbers ranging from 0.2 to 0.7 and angle of attack values of 3, 5, 8, and 12 degrees [39].

The pressure coefficient was used to analyze the pressure differential above and below the aero foil, which affected the lift values. The lift-to-drag ratio is an important design criterion for aero foil performance. Modal analysis was conducted to study the natural characteristics, mode shapes, and vibration frequencies of the aero foil [40].

The paper presented a conceptual study using CFD to explore alternate methods for stall control and lift-to-drag improvement in airfoils. Three passive devices were examined: Stall vane,

Cylinder, and Dimples. The first device, Stall vane, eliminates separation at 15 degrees of angle-of-attack but increased total drag by 22%. The main element drag, however, reduced by 43%. The maximum lift coefficient remains unchanged. The second device, Cylinder, causes flow separation and significantly decreased the lift-to-drag ratio at a given lift coefficient [41].

The third device, Dimples, shows potential for improving the lift-to-drag ratio at higher angles-of-attack, but further investigation was required. Experimental data was compared with CFD results to validate the computational model. The paper highlighted the motivation to study effective techniques for performance improvement with fewer drawbacks than existing methods [42].

The paper focused on a conceptual study of performance enhancing devices for an airfoil using CFD. Two simple passive devices are selected and examined for lift improvement and drag reduction. The CAD model was prepared in CATIA V5 R19, pre-processing done in ANSYS ICEM CFD 14.0, and simulations was carried out in ANSYS FLUENT 14.0 [43].

The aim of the project was to improve airfoil performance at high angles of attack. The study used factorial design on Design of Experiment methods to reduce the number of combinations for simulation. Lift and drag coefficients, as well as the lift-to-drag ratio, are analyzed. The study identified the optimum position for placing dimples and cylinders to enhance airfoil performance [44].

The NASA Tetrahedral Unstructured Software System (TetrUSS) is a package of software used for aerodynamic analysis, including grid generation and flow solutions. TetrUSS has been used in high priority NASA programs and has won the NASA Software of the Year Award twice .The TetrUSS package includes software packages such as GridTool for preparing geometries for grid generation, VGRID for generating unstructured grids, and USM3D as the flow solver [45].

GridTool can read NURBS curves and surfaces and allows users to define surface patches and control grid spacing parameters .VGRID is used for unstructured grid generation, including the generation of viscous layers and the in viscid portion of the volume grid. USM3D is a parallelized, tetrahedral cell-centered, finite volume Reynolds Averaged Navier-Stokes (RANS) flow solver with various turbulence models implemented [46].

The paper proposes a novel multi-output neural network for predicting aerodynamic coefficients of aero foils and wings, which is compared with other approaches found in the literature. The paper also presents a detailed comparison of the proposed neural network with the popular proper orthogonal decomposition (POD) method. The numerical results show the benefits of the proposed approach in high dimensional problems with flow and geometric parameters. The paper mentions the use of the singular value decomposition of the snapshot matrix and the vector of conservation variables and flux tensor in the context of neural networks [47].

The paper compares three neural networks, where the first network considers inputs M and a, and the lift, drag, or moment coefficient as a single output. The paper compares the proposed approach to the POD method in numerical examples involving parameterized inflow conditions and geometries. **[**The paper presents surface pressure contour plots and comparisons between the full order and neural network predictions, showing good visual agreement. The paper discusses the accuracy of the neural network predictions for different inflow conditions, with the third network showing higher accuracy [48].

CHAPTER 3

MATHEMATICAL MODELING

This section includes all the mathematical formulas and calculations which were carried out to get the final prototype model prepared. A detailed explanation, both mathematical and theoretical is included here.

The fundamental component of an airplane that keeps the craft in the air is its wing. Wings are responsible for many important tasks, for instance, lift generation, stability and control during flight, for entire aircrafts structural support and sometimes fuel storage. The lift generated is controlled by the wing shape known as the airfoil.

There are various configurations of the aero foils such as flat bottoms, under-cambered, symmetrical or semi-symmetrical, and many more. This aircraft is blend of two aero foils, first of which is 1) a reflex airfoil and 2) an under cambered airfoil [49].

The following calculations were carried out before manufacturing the prototype:

3.1 WING CHARACTERSTICS

The body weight of an airplane is the most fundamental factor that determines the size of its wings. The wing of the plane plays a very crucial part in lift generation. Also it helps greatly in maintaining the stability of plane. Some planes wing also has the ability of storing fuel in the wing section.

Maximum speed, cruising efficiency, and range are only a few of the performance aspects that are impacted by the wing design. Depending on the intended use and mission of the aircraft, several wing shapes and configurations are used. Their size, shape, and design are extremely important factors.

A plane needs to produce lift that is at least as great as its weight in order to take off and maintain flight. Consequently, including lift that is a little bit larger than the weight and coefficient of lift value of the chosen airfoil equation, we can easily find out how much wing area is needed. Therefore,

Wing area (S) =0.3845 m^2

$lift = 1/2 \times p \times v^2 \times CL \times S$ … ... (1)

Where,

- Wing area (S) =0.3845 m^2
- Lift required (L) =1.5 kg×9.8 ms^{-2}
- Density of air (p) = 1.225 kgm^{-3}
- Cruise velocity (v) = 25 ms^{-1}

Putting all values in equation (1), we get the coefficient of lift as:

Coefficient of lift (C_L) = 0.0998

The lift coefficient (C_L), which is a dimensionless quantity in fluid dynamics, connects the lift produced by a lifting body to the fluid density surrounding it, the fluid velocity, and a related reference region. It is an essential variable that aids engineers and designers in understanding an airfoil's lift properties and enhancing its performance.

The coefficient of lift allows engineers and designers to compare lift generation across various aircraft and configurations at varying angles of attack since it takes the aerodynamic characteristics of the airfoil or wing into consideration.

A fixed-wing airplane is an example of a lifting body, as is a foil or a whole foil-bearing body.

Table 1: Wing parameters (a)

WING PARAMETERS	
Wing area (S)	0.3845 m^2
Lift (L)	1.5 kg×9.8 ms^{-2}
Density of air (p)	1.225 kgm^{-3}
Cruise velocity (v)	25 ms^{-1}
Coefficient of lift (C_L)	0.0998

After the calculations and putting values in the above mentioned equations, the results came out as mentioned in the table 1(a).

3.2 ASPECT RATIO (AR)

The ratio of an aero foil's length to average surface width is known as the aspect ratio. For aircraft wings, the aspect ratio is a key design factor since it has a big impact on the wing's aerodynamic properties.

The three categories of aspect ratios are low aspect ratio, medium aspect ratio, and high aspect ratio and its magnitude depends on the type of aircraft. A higher aspect ratio means generation of more lift and correspondingly more efficiency. The aspect ratio of a wing is the proportion of the wing length to the average chord length.

Aspect Ratio (AR) = Span/Chord length … … (2)

Where,

- Span=1.8288 m
- Chord length= 0.5842 m

Putting the above mentioned values in equation (2)

Aspect Ratio = 3.1304

- Span= Area× AR… ... (3)

  =1.8288 m

- Chord length (MAC) =AR× Span… ... (4)

  =0.5842 m

- Root Chord (Cr) =2× S/ [Span (1+ lambda)] … …(5)

  =0.5842 m

Table 2: Wing parameters(b)

WING PARAMETERS	
Aspect ratio	3.1304
Span	1.8288 m
Chord length	0.5842 m
Root chord	0.5842 m

The aspect ratio, span, chord length and root chord turned out to be 3.1304, 1.8288m, 0.5842m and 0.5842m respectively.

3.3 WING LOADING (W.L)

Wing loading in aerodynamics is calculated by dividing an aircraft's total mass by the area of its wings. An aircraft's wing loading affects its stalling speed when it is flying straight and level. The weight and projected area of the wings are the only two parameters that affect wing loading, but it also has an impact on an aircraft's ability to turn and its stability [50].

Insights into an aircraft's performance characteristics, such as takeoff and landing speeds, climb rate, fuel efficiency, maneuverability, and stability, can be gained from knowing its wing loading. It is a crucial factor in the design and operation of airplanes.

Wing loading= Weight/Area… ... (6)

Where,

- Weight= 1.5 kg

Putting values in equation (6),

Wing loading=1.5 kg /0.3845 m^2

=3.90117

Table 3:Wing Loading

WING LOADING	
Weight	1.5 kg
Wing loading	3.90117 kgm^{-2}

The weight of the craft was 1.5 kg and the wing loading was 3.90117 kgm^{-2} after calculating and putting values in equation (6).

3.4 ELEVONS

An aileron and an elevator both have the same purpose as an elevon. An elevon is a mixture of both the aileron and elevator. The single both replacing the two components basically help in reducing weight and saves the fuel effectively by performing exactly the same job. The trailing edge of the wings has movable control surfaces called elevon.

At the trailing edge of the wing, elevons are mounted on each side of the aircraft. These elevons are used for controlling yaw movement and cause pitch up and pitch down. To supply the proper position for each elevon, the inputs of the two controllers are combined mechanically or electrically [51].

Its application necessitates careful consideration of aerodynamics, stability, and control efficiency. Elevons must be designed and tested properly in order to give the appropriate control authority and stability without jeopardizing the aircraft's performance and safety.

Elevon =12% × Wing Area… ... (7)

=12× 0.3845 m^2

=0.04614 m

Chord length=Span/AR…. ... (8)

=1.8288 m/3.1304

=0.584 m

Chord length of Elevon = 0.584×20%… ... (9)

=0.1168m

Table 4: Elevons

ELEVONS	
Elevons length	0.4614 m
Chord length	0.1168 m

These values were calculated for elevons. Elevons length was 0.4614 m and chord length turned out to be 0.1168 m.

3.5 REYNOLDS NUMBER

Reynolds number, a dimensionless quantity, is used to categorize the flow pattern through a pipe as laminar or turbulent. The ratio of inertial to viscous forces determines the Reynolds number. Laminar flow is defined as having a Reynolds number less than 2000 and turbulent flow as having a Reynolds number greater than 4000.

Because it affects an aircraft's aerodynamics, drag, stall behavior, flying parameters and in short, overall efficiency, the Reynolds number is a crucial aviation metric and must be selected very carefully. The Reynolds number is a tool used by engineers and designers to forecast performance, improve safety, and assure efficient and safe flying.

Reynolds Number (Re No.) = p× v ×chord length/viscosity… ... (10)

Where,

- P=1.225 kgm^{-3}
- Chord length=0.584 m
- v= 25 ms^{-1}

- Viscosity=1.81×10^{-5}

$=1.225\times25\times0.584/1.81\times10^{-5}$

$=988121.547$

Table 5: Reynolds Number

REYNOLDS NUMBER	
Viscosity	1.81×10^-5 Nsm^{-2}
Reynolds number	988121.547

The Reynolds number for the air was selected as 988121.547 and the air viscosity was 1.81×10^-5 Nsm^{-2} which is actually the standard air viscosity.

3.6 THE FUSELAGE

The primary body part of an airplane is called the fuselage. It accommodates personnel, travelers, or freight. Although in some amphibious aircraft the single engine is installed on a pylon attached to the fuselage, which is then used as a floating hull, in single-engine aircraft it will typically also contain an engine. Depending on the type of aircraft and its intended usage, fuselages come in a variety of shapes and layouts.

To meet particular design needs, they can have complex shapes like ellipses or cylinders. Various avionics systems, wiring, and equipment required for navigation, and communication are housed in the fuselage. The aircraft's fuselage gives it stiffness and structural strength. In doing so, it distributes the aerodynamic loads and supports the weight of the aircraft as it joins the wings, tail, and other parts.

Fuselage=75%× span… ... (11)

=75×1.8288 m

=1.3716 m

Height =9%× fuselage… ... (12)

=0.09× 0.0148 m

=0.001332 m

Table 6: Fuselage Characterstic

FUSELAGE	
Fuselage	1.3716 m
Height of fuselage	0.001332 m

For the fuselage, its length, after putting values into the formula and selecting 75 percent of span came out to be 1,3716m and its height as 0.001332m.

After calculating all the required parameters, the 3D printed model and the final prototype was manufactured according to above mentioned values.

CHAPTER 4

DESIGN METHODOLOGY

4.1 PRELIMINARY STEPS

In order to get the prototype model prepared, there was a series of experiments and different designing steps to ultimately meet the final goal and get the desired blended wing prepared. In the sequence of different designing steps, the very initial step was to model a scale down version of blended wing aircraft. This model was manufactured with specific dimensions which could perfectly fit inside the wind tunnel and go through a series of different wind tunnel experiments to get the results at different wind velocities and angle of attack. Afterwards, the main prototype was manufactured.

First of all, for the blended wing aircraft, it holds a great significance to select such aero foils which could fit best to the problem statement and the criteria. As it is a blend of two aero foils, hence two unique aero foils are to be selected. To fulfill the criteria of low speed and low Reynolds number, these were the two aero foils which were best fitting to the scenario:

4.1.1. AEROFOIL SELECTION

4.1.2. MH78-A REFLEX AERO FOIL

MH78 is a reflex airfoil, which means the trailing edge of the aero foil is slightly upward as compared to the leading edge and hence has a positive pitching moment and mainly used in tailless configurations such as blended wing. Reflex aero foils often have a trailing edge that slopes downward, which helps improve its longitudinal stability. The MH78 aero foil is frequently utilized in a variety of low-speed and high-lift applications because of its exceptionally good low-speed performance. Following are some notable feature of this wing profile:

1. It has a modest amount of camber and a reasonably thick profile, which enable it to provide significant lift at low speeds.

2. The aero foil's high lift properties make it ideal for uses where the device or aircraft needs to provide enough lift to take off and land slowly. As a result, it is only used in flying wing and tailless aero planes.
3. It has a thick and round leading edge that helps in accommodating maximum passengers.
4. It has a maximum thickness of 14.4% at 22.1% chord and maximum camber of 1.9% at 17.9% chord length.
5. High lift-to-drag ratios are the goal for blended wing aircraft in order to increase range and fuel efficiency which is one of the characteristics of MH78.

Hence, based on above mentioned properties this was the most optimum selection for the fuselage.

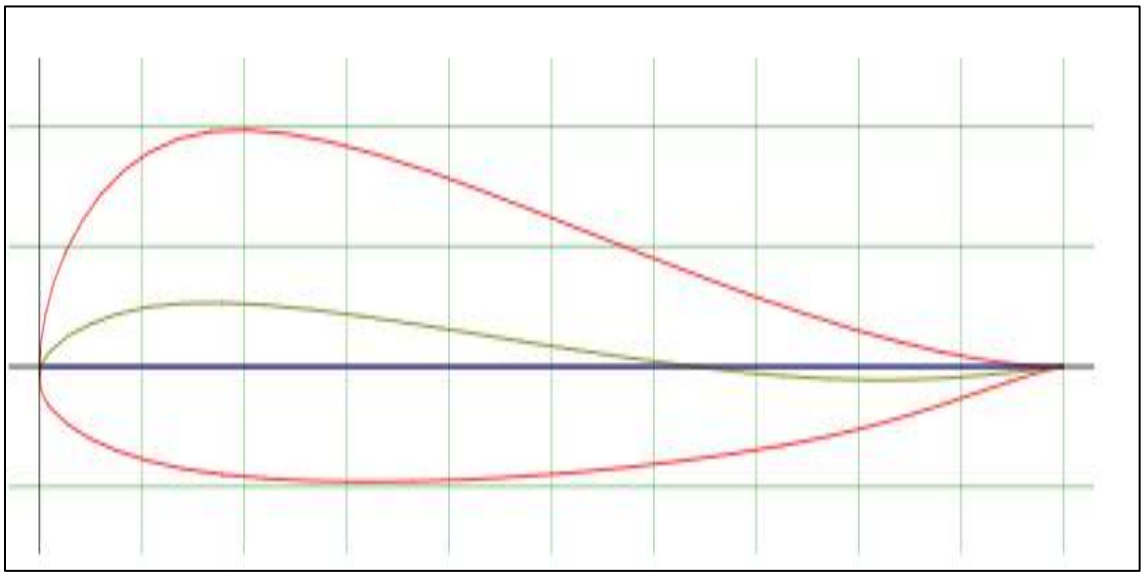

Figure 3: MH78 PROFILE

4.1.3. S1223-AN UNDER CAMBERED AERO FOIL

This is an under cambered aero foil, also termed as symmetric airfoil. This is one of the most optimized aero foils to be used at low speed and low Reynolds number as it owns the capability of generating higher lift values at lower speeds as well. Hence Selig S1223

is said to be best regarded aero foil for low-speed applications. Following is some technical details of this profile:

1. A medium camber and a rather slender profile define the Selig S1223 aero foil.
2. It is suited for a variety of applications where low-speed performance is required since it has been specifically created to deliver advantageous lift and drag characteristics at low speeds. More specifically, this helps in landing and takeoff time of the craft.
3. A predictable and controllable stall behavior is made possible by the S1223 airfoil's moderate stall behavior and smooth airflow separation. For low-speed flight to remain stable and under control, this is crucial.
4. This aero foil is designed in such a way to reduce drag, which automatically reduces fuel consumption.
5. It has a maximum thickness of 12.1% at 19.8% chord and a maximum camber of 8.1% at 48% chord.

As the project is also based on low speed analysis, therefore this is the most suitable second wing profile for the span of the craft.

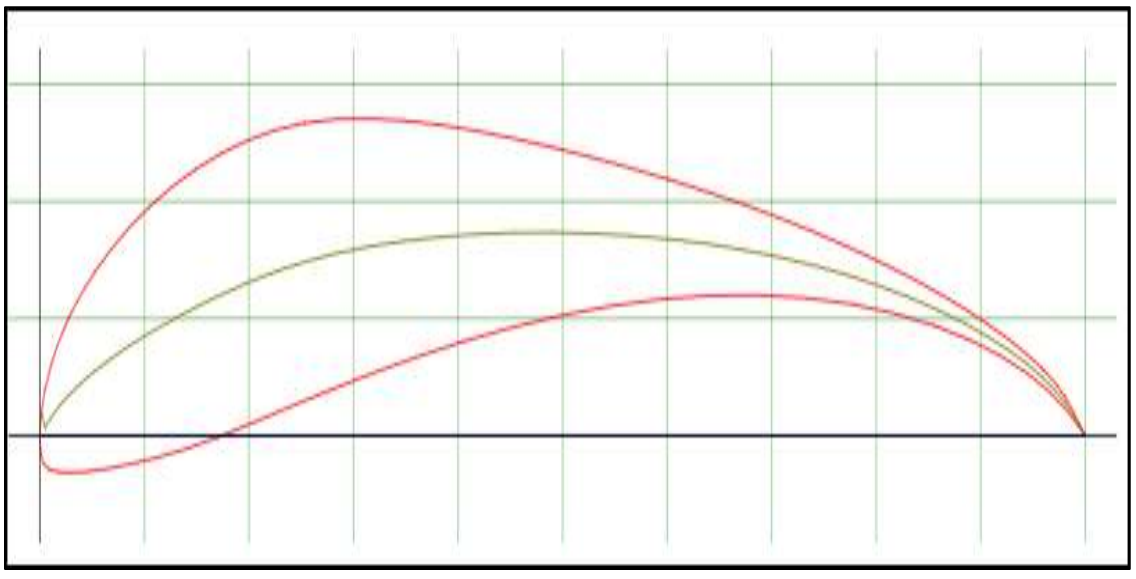

Figure 4: S1223 aero foil

4.2 WING CONFIGURATION

There are different configurations of wing which includes straight wing, swept wing, delta wing, tapered wing, elliptical wing, swept-back tapered wing and similarly many more other configurations exists. This projects craft is a back swept blended wing configuration. Different wing configurations have different performance behavior, aerodynamic behavior and likewise stalling behavior at different speeds and different angle of attacks. For instance, a straight wing has a capability of stalling at lower angle of attack. This angle is commonly referred as critical angle of attack [52].

The range of critical angle for straight wing lays between15 degrees to 20 degree. Whereas, at greater angles of attacks, a swept wing, which has its leading edge, swept back, is more likely to stall. Its critical angle varies from the range of 20 degrees to 35 degrees but it is not just confined to attacking angles rather many other features adds into the stability characteristics.

The other parameter includes the airfoil shape used as well as various aerodynamic devices also control the stalling of craft. Due to their many benefits at greater speeds, swept wings are frequently utilized in high-speed aircraft and blended wings. In contrast to straight wings and many other similar wing profiles, swept wings may exhibit a more abrupt and less smooth stall behavior at lower speeds and greater angles of attack. Hence the selection of back swept is mainly done to make the craft more stable in order to avoid stalling behavior and to achieve specific performance goals.

4.3 WING WASHOUT

Wing washout, which is also frequently known as twist angle, helps in controlling and predicting more stable behavior and aerodynamic characteristics of aircraft. This is actually a twist at the angle of incidence of the wing. Also, the aircraft's roll stability is greatly influenced by washout. When one wing begins to stall, the other wing, which is still flying, produces more lift as a result. The tendency for the aircraft to roll uncontrollably during a stall is lessened by this differential lift, which also aids in gently leveling the wings. Washout can also make the aircraft's controls more responsive.

The primary reasons of adding wing twist into a plane is that, firstly it adds to the stability during flight operation and side by side helps to balance lift distribution across the wing area. It helps in opposing stall behavior as the reduced lift can ultimately result to the crash of plane. But due to adding twist angle, the wing root has a delayed stalling behavior than wing tip and ultimately helping in reducing chances of any calamity [53].

The blended wing body used in this project includes a washout angle which is a negative twist angle of -3 degrees. Just like a washout, there is also another similar designing technique which is referred as wing wash in. The basic difference in wash in and wash out is that they both are twisting in the wing but in opposite direction. The wing wash in is not suitable for low planes rather its requirement is more needed and appreciated in high speed aircrafts. As this plane is a subsonic speed blended wing body, which means its speed is lower than the speed of sound, which is why the use of washout is more feasible and effective over here.

4.4 WINGLETS

At the extreme point of an airplane's wings, the winglets are located, which are one of the most important aerodynamic devices used in designing the craft. They are small vertical extensions that occasionally point upward or downward and have multiple functions to enhance the effectiveness and performance of aircraft.

There are many benefits of winglets, some of which are mentioned ahead. First of all, these winglets perform a great job in overcoming and reducing the induced drag. Induced drag is produced when the aero plane generates lift and as a result of this, there is formation of vortices at the tip of wing. The relation between the induced drag and air craft’s speed is inversely related. The magnitude of this induced drag depends upon many parameters like the amount of lift produced, the aspect ratio kept, and area of the wing, lift distribution across the wing and wing loading [54].

This induced drag is basically the formation of vortices at the tip of wing which causes energy loss and also greatly affects fuel efficiency which is not a desired parameter. Secondly, when this induced drag is reduced, automatically the losses which could be caused by it vanish and it correspondingly enhances the fuel efficiency [55].

The winglets also add to the lateral stability by increasing the aspect ratio of the wing. Winglets can also improve an aircraft's performance during takeoff and ascent by lowering the power needed during these crucial flight periods. When the aircraft's performance is at its lowest and at high altitudes or in hot weather, this can be extremely helpful. Winglets are not a must aerodynamic device. Rather it is added just for the core reason of enhancing the efficiency of craft. Also for long flight and less fuel consumption, they play a very significant role.

4.5 3D PRINTED MODEL

In the process of testing and experimentation, prior to making the actual prototype, firstly a small scale down model was prepared to be used for testing in the wind tunnel, ESSOM-ISO 9001, for testing at different wind velocities and angle of attack. This small BWB was modeled on SOLID WORKS software and afterwards 3D printing was carried out.

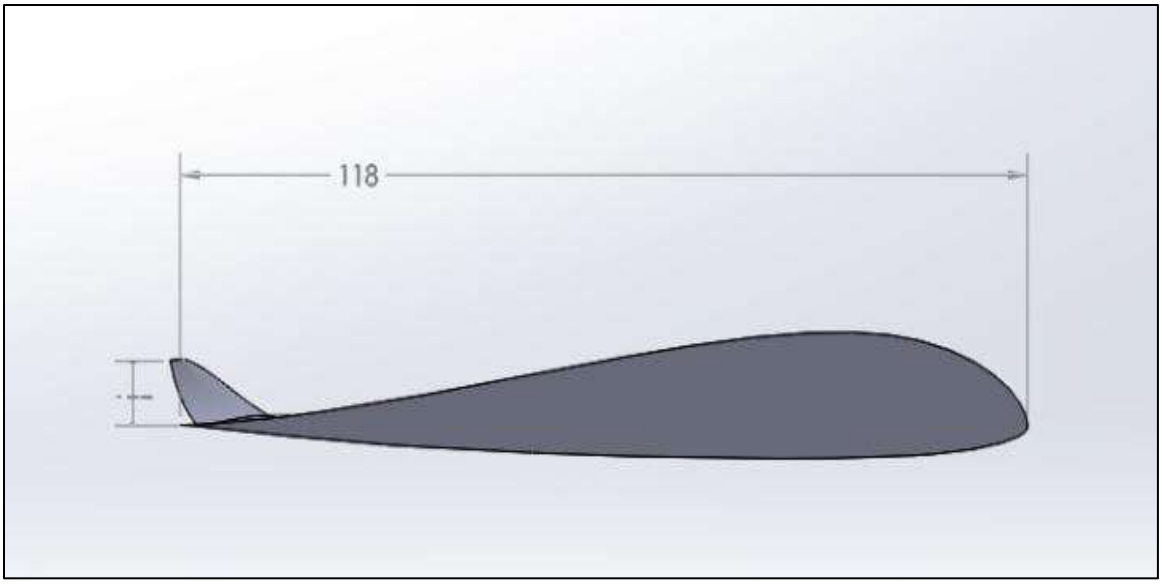

Figure 5: SOLIDWORKS model dimensions (a)

These are the views for different sections of the small scale down model of the blended wing for experimentation process.

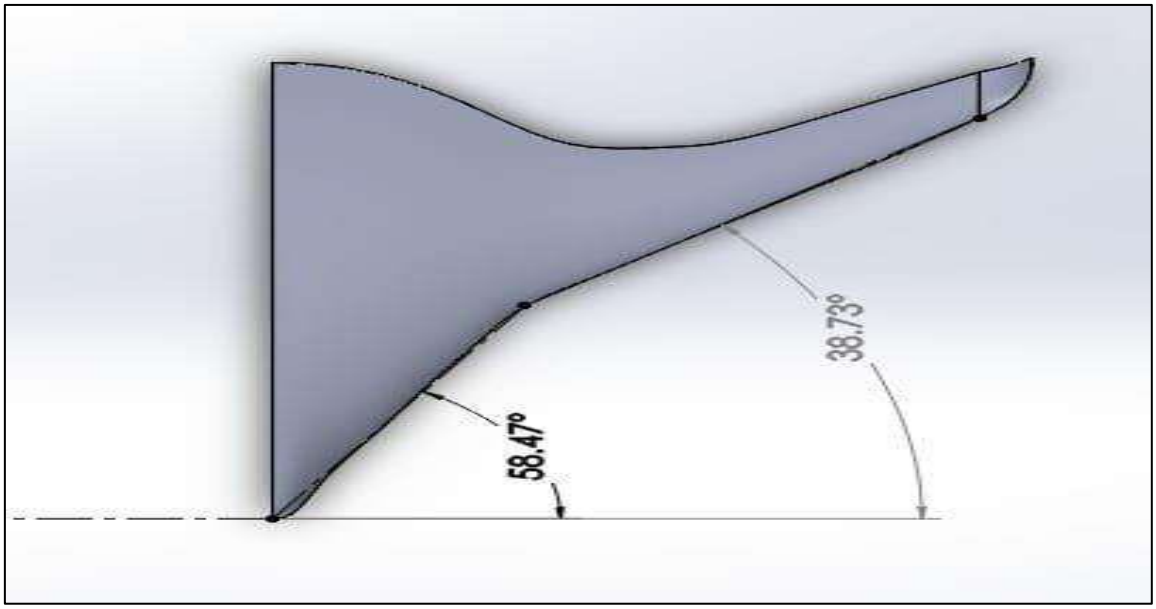

Figure 6: SOLIDWORKS model dimensions (b)

This is the top view of the SOLIDWORK scaled down model and dimension of its span from one wingtip to the other one.

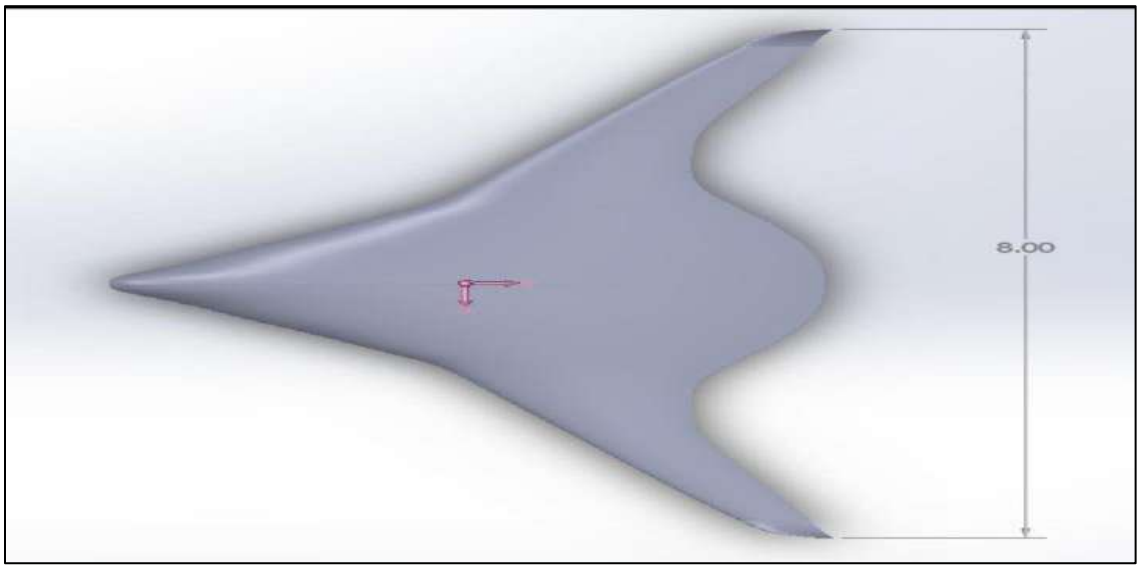

Figure 7: SOLIDWORKS model dimensions (c)

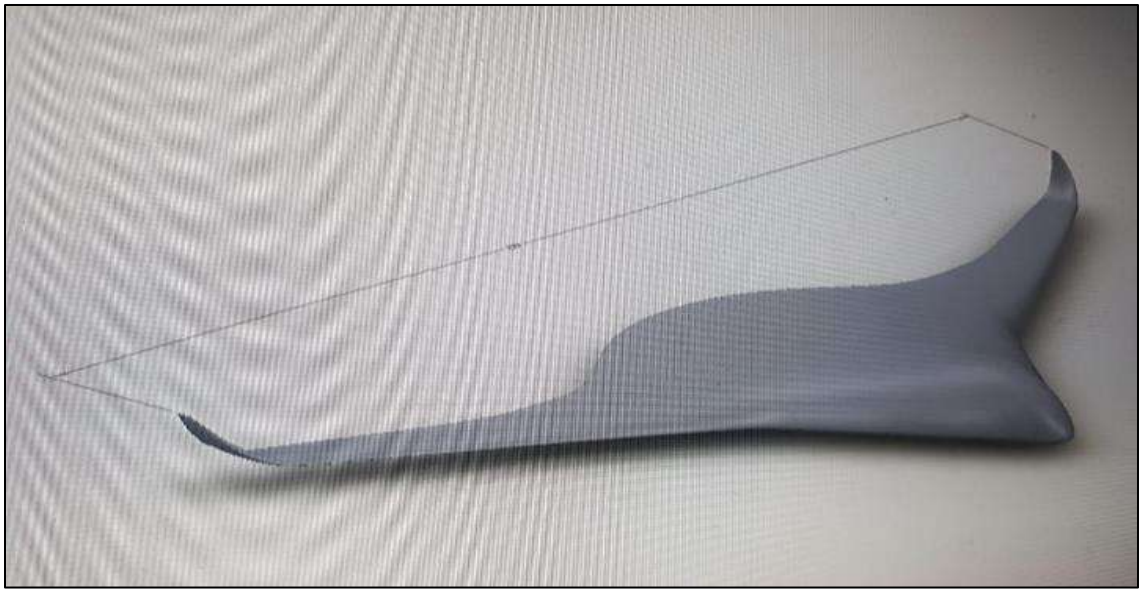

Figure 8: SOLIDWORKS final model

Once this model was prepared, it was 3D printed afterward. The final product was as following:

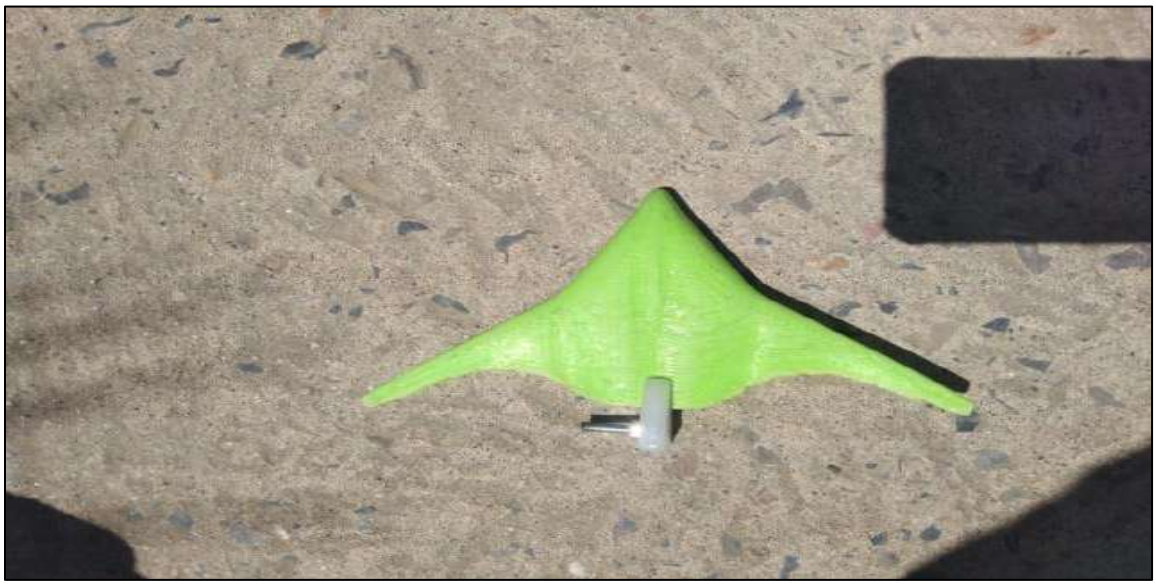

Figure 9: 3D printed model (a)

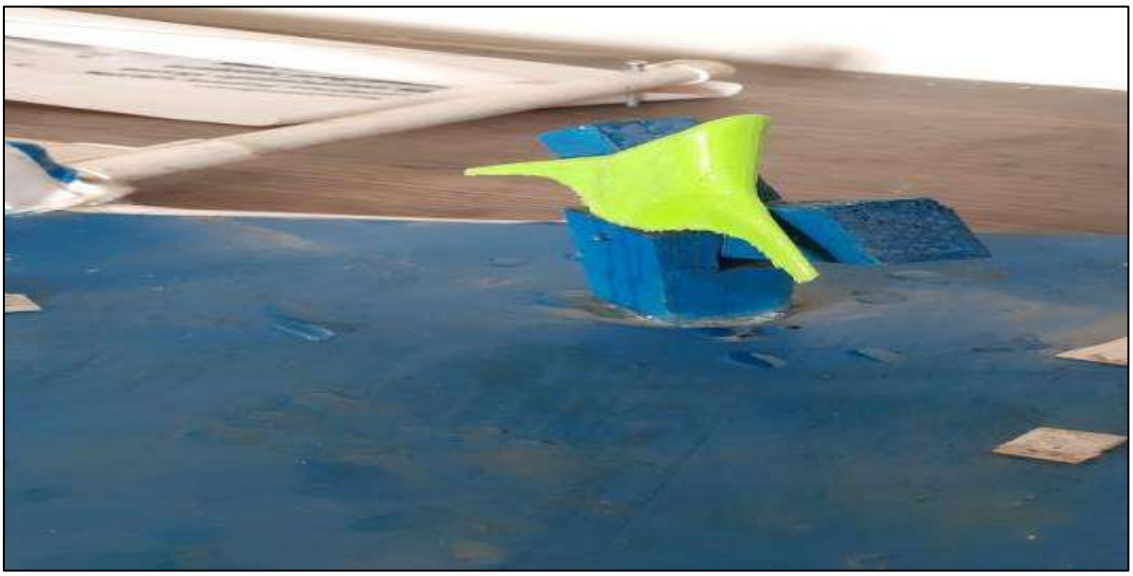

Figure 10: 3D printed model (b)

This model was afterwards tested in the wind tunnel to get the experimental results and later on the data was compared with the simulated data. This 3D printed model was fitted inside the wind tunnel by adding a screw so that the holder could hold it tightly and it does not leave its position while the wind is passed through it. This was the wind tunnel used:

Figure 11: Wind tunnel ESSOM

This was the small model of blended wing attached inside the wind tunnel and ready for the testing process. It was initially attched at zero degree of angle of attack.

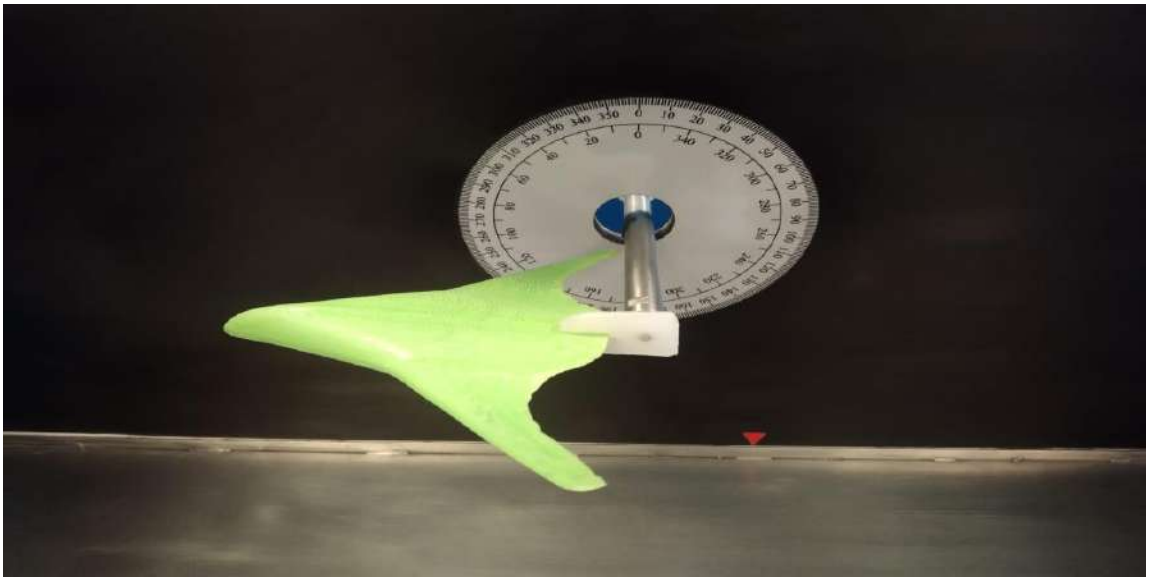

Figure 12: Testing chamber wind tunnel at angle 0^0 (a)

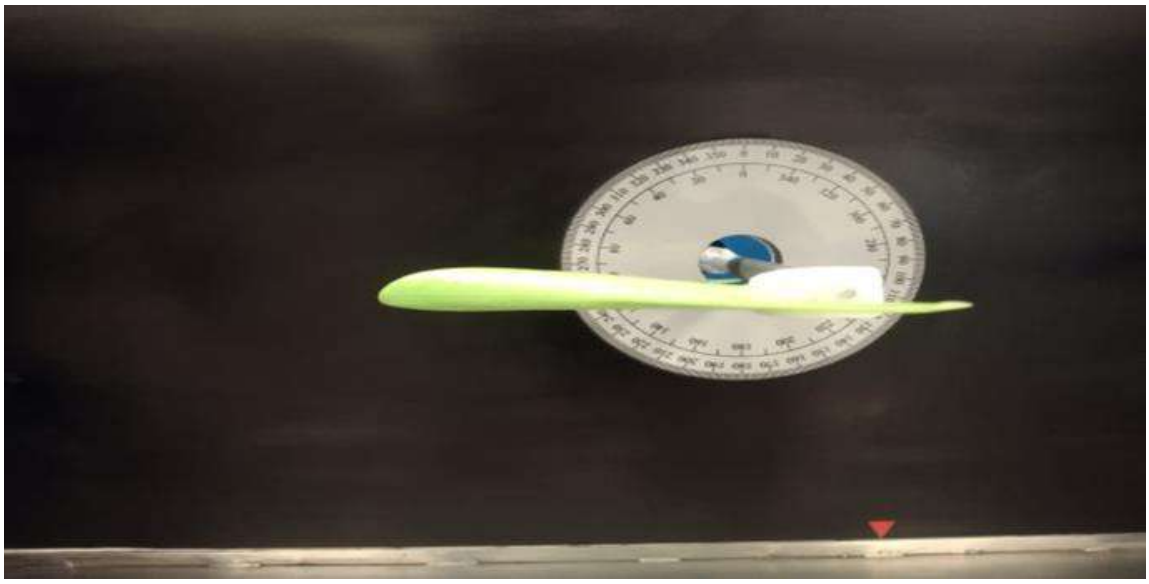

Figure 13: Testing chamber wind tunnel 0^0 (b)

After fixing it rigidly and properly inside the testing chamber of the wind tunnel, the experimentation process was started. Firstly, a particular wind velocity was set and correspondingly different angle of attack ranging from 0 degrees to 15 degrees were changed to check the results for lift, drag, pitching moment, coefficient of lift and coefficient of drag. The velocity was set as 10 ms^{-1}. Gradually the speed was increased to 20 ms^{-1}, 30 ms^{-1} and ultimately 40 ms^{-1}. At these wind velocities, magnitude of the required aerodynamic parameters was analyzed.

After completing this step, next the angle of attack was kept constant and correspondingly the wind velocity was increased from 0 ms^{-1} to 30 ms^{-1}. It included an increment of 10 every time and just like previous testing, the changes in all those aerodynamic parameters were checked.

4.6 ANSYS WORKBENCH SIMULATIONS

After the results were taken and all the desired aerodynamic data was collected from wind tunnel testing, next step was to perform analysis on ANSYS software. Hence after the IGS file was imported from SOLIDWORKS to ANSYS WORKBENCH, the simulations were started. An enclosure was made on the software and inside, the model was kept.

It was actually imitating the same wind tunnel chamber and putting the same solid geometry which was previously tested on wind tunnel. After entering all the required data and keeping fluid was air, the simulations were done for velocity 40 ms^{-1}. Once the simulations were done, all the desired aerodynamic parameters including coefficient of lift, coefficient of drag, velocity contours and pressure contours were collected.

The results of experimentally done wind tunnel testing and simulations performed on ANSYS WORKBENCH were later on compared with each other in order to calculate the error and predict the efficacy of the manufactured blended wing body, amalgam of MH78 and S1223.

CHAPTER 5

RESULTS AND DISCUSSION

After the experimentation process, on the wind tunnel and the simulations performed on ANSYS WORKBENCH, the results were gathered to find weather this new prototypes is a better option for future aircrafts or not. Following is a descriptive form including the tables, diagrams and graphs acquired during the testing process:

5.1 WIND TUNNEL EXPERIMENTATION RESULTS

Initially the wind velocity was kept constant while the angle of attack was gradually increased. Here is some basic information about different parameters

- Wind tunnel testing chamber area = $0.18m^2$
- Air density = $1.225\ kgm^{-3}$
- Coefficient of lift = $2F_L/(\rho \times v^2 \times Area)$… … (13)
- Coefficient of drag = $2F_D/(\rho \times v^2 \times Area)$… … (14)

Following table show different parameters for varying wind speeds:

Table 7: Results for 10 ms^{-1}

ANGLE OF ATTACK (^{0})	**LIFT (N)**	**DRAG (N)**	**PITCHING MOMENT COEFFICIENT**	**AIR VELOCITY (ms^{-1})**	**COEFFICIENT OF LIFT**	**COEFFICIENT OF DRAG**
0	0.02	0	-0.0	13.5	0.001840	0
5	-0.02	-0.01	0.001	12.1	-0.001840	-0.0009070
10	-0.01	0	0.001	10.7	-0.0009070	0

15	-0.02	-0.01	0.001	9.9	-0.0018140	-0.0009070
20	-0.02	-0.02	0.001	9.6	-0.0018140	-0.0018140

According to the results in the above table which were calculated in the wind tunnel for speed 10 ms^{-1}, the results show a valid behavior as the positive lift is generated till 3 degrees and then the lift value starts coming in negative direction. Hence after 3 degrees the plane couldn't generate enough lift for flight.

Table 8: Results for 20 ms^{-1}

ANGLE OF ATTACK (^{0})	**LIFT (N)**	**DRAG (N)**	**PITCHING MOMENT COEFFICIENT**	**AIR VELOCITY (ms^{-1})**	**COEFFICIEN OF LIFT**	**COEFFICIENT OF DRAG**
0	0.08	-0.01	0.001	0	0.0018140	-0.00022675
5	0.01	-0.05	0.001	0	0.00022675	-0.0011337
10	0.02	-0.01	0.001	0	0.00045351	-0.00022675
12	0.02	-0.01	0.001	0	0.00045351	-0.00022675
15	-0.02	-0.04	0.001	0	-0.0004535	-0.00090702
18	-0.04	-0.06	0.001	0	-0.0009070	-0.0013605
20	-0.04	-0.03	0.001	0	-0.0009070	-0.00068027

For 20 ms^{-1} wind velocity, the results show a positive lift value till 12 degrees which again show a very positive behavior. At this low speed, the plane, still, was able to generate enough lift for maintaining good flight but after 12 degrees again the lift started getting less.

Table 9: Results for $25ms^{-1}$

ANGLE OF ATTACK (^{0})	**LIFT (N)**	**DRAG (N)**	**PITCHING MOMENT COEFFICIENT**	**AIR VELOCITY (ms^{-1})**	**COEFFICIENT OF LIFT**	**COEFFICIENT OF DRAG**
0	0.09	-0.02	0.002	0	0.0013061	-0.00029024
5	0.05	-0.04	0.002	0	0.00072562	-0.00058049
10	0.04	-0.01	0.002	0	0.00058049	-0.00014512
12	0.02	-0.02	0.002	0	0.00029024	-0.00029024
15	-0.01	-0.03	0.002	0	-0.00014512	-0.00043537
18	-0.06	-0.05	0.002	0	-0.00087074	-0.00072562
20	-0.06	-0.04	0.002	0	-0.00087074	-0.00058049

The lift for 25 ms^{-1} was generated till 12 degrees again but the lift remained positive for some more angle of attack before getting its value reduced. As the speed is increasing for the craft, similarly lift is also acting directly with it hence proving a blended wing to be more efficient.

Table 10: Results for 30ms^{-1}

ANGLE OF ATTACK (^{0})	LIFT (N)	DRAG (N)	PITCHING MOMENT COEFFICIENT	AIR VELOCITY (ms^{-1})	COEFFICIENT OF LIFT	COEFFICIENT OF DRAG
0	0.17	-0.02	0.002	0	0.001713	-0.0002015
5	0.10	-0.05	0.002	0	0.0010078	-0.0005039
10	0.09	-0.01	0.002	0	0.00090702	-0.00010075
12	0.06	-0.02	0.002	0	0.0006046	-0.0002015
15	0.03	-0.04	0.002	0	0.0003023	-0.00040312
18	-0.01	-0.07	0.002	0	-0.00010078	-0.0007054
20	-0.02	-0.06	0.002	0	-0.0002015	-0.0006046

For 30 ms^{-1} and 15 degrees of angle of attack, the lift is generated more as compared to previous air speed where at 15 degrees, the results show a negative lift value but here, it is giving positive lift for 15 degrees as well. A normal conventional plane usually stalls after 12 degrees but a blended wing is still giving sufficient lift.

Table 11: Results for 35ms^{-1}

ANGLE OF ATTACK (^{0})	LIFT (N)	DRAG (N)	PITCHING MOMENT COEFFICIENT	AIR VELOCITY (ms^{-1})	COEFFICIENT OF LIFT	COEFFICIENT OF DRAG
0	0.22	-0.03	0.002	0	0.001628	-0.0002221
5	0.14	-0.06	0.002	0	0.001036	-0.0004442

10	0.11	-0.02	0.002	0	0.0008144	-0.0001481
12	0.19	-0.02	0.002	0	0.001406	-0.0001481
15	0.05	-0.05	0.002	0	0.0003702	-0.0003702
18	-0.01	-0.07	0.002	0	-0.00007404	-0.0002591
20	-0.02	-0.07	0.002	0	-0.000148	-0.0002591

The lift value is still positive and getting higher with increasing speed for the same angle of attack and after 16 degrees its value shows a negative lift value.

Table 12: Results for 40 ms^{-1}

ANGLE OF ATTACK (^{0})	**LIFT (N)**	**DRAG (N)**	**PITCHING MOMENT COEFFICIENT**	**AIR VELOCITY (ms^{-1})**	**COEFFICIENT OF LIFT**	**COEFFICIENT OF DRAG**
0	0.29	-0.05	0.002	0	0.001643	-0.0002834
5	0.20	-0.07	0.002	0	0.00113	-0.0003968
10	0.15	-0.03	0.002	0	0.0008503	-0.00017
12	0.13	-0.02	0.002	0	0.0007869	-0.0001133
15	0.07	-0.06	0.002	0	0.0003968	-0.0003401
18	0.01	-0.09	0.002	0	0.00005668	-0.0005102
20	-0.04	-0.09	0.002	0	-0.002267	-0.0005102

This table is a prove for the blended wing to be a more efficient and improved design for the future crafts as the lift value appears even for 18 degrees and after 18 degrees the planes lift starts getting low again.

Next experiment was to keep angle of attack constant while velocity was varied gradually. Following results were given by wind tunnel:

Table 13: Results for 5° AOA

VELOCITY (ms^{-1})	**LIFT (N)**	**DRAG (N)**	**PITCHING MOMENT COEFFICIENT**	**AIR VELOCITY (ms^{-1})**	**COEFFICIENT OF LIFT**	**COEFFICIENT OF DRAG**
5	0.03	0.02	-0.00	18.8	0.000769	0.000513
10	0.06	0.03	-0.00	18.7	0.001539	0.000769
15	0.13	0.07	-0.00	18.8	0.003336	0.001796
20	0.23	0.11	-0.00	18.7	0.005902	0.002822
25	0.39	0.18	-0.00	18.7	0.010008	0.004619
30	0.59	0.26	-0.00	18.8	0.0151411	0.0066723

For 5 degree angle of attack, as the air velocity is increased, so is the corresponding lift increasing as evident from the table as well.

Table 14: Results for 10 AOA

VELOCITY (ms^{-1})	**LIFT (N)**	**DRAG (N)**	**PITCHING MOMENT COEFFICIENT**	**AIR VELOCITY (ms^{-1})**	**COEFFICIENT OF LIFT**	**COEFFICIENT OF DRAG**
5	0.02	0.01	-0.00	18.7	0.0005132	0.0002566
10	0.08	0.01	-0.00	18.7	0.002053	0.0002566
15	0.18	0.04	-0.00	18.8	0.0046193	0.001026
20	0.35	0.10	-0.00	18.5	0.0089820	0.002566
25	0.63	0.22	-0.00	18.6	0.01616	0.005645
30	0.91	0.31	-0.00	18.7	0.023353	0.007955

The relation between the velocity of air and lift is directly related. Therefore, if the velocity is increased, proportionally will the lift increase as well.

Table 15: Results for 15 AOA

VELOCITY (ms^{-1})	**LIFT (N)**	**DRAG (N)**	**PITCHING MOMENT COEFFICIENT**	**AIR VELOCITY (ms^{-1})**	**COEFFICIENT OF LIFT**	**COEFFICIENT OF DRAG**
5	0.06	0.04	-0.00	18.7	0.001539	0.001026
10	0.14	0.08	-0.00	18.7	0.003631	0.002053
15	0.29	0.14	-0.00	18.5	0.007522	0.003631

20	0.54	0.25	-0.00	18.5	0.01385	0.006484
25	0.89	0.38	-0.00	18.6	0.02283	0.009751
30	1.25	0.54	-0.00	18.7	0.03207	0.01385

Again the direct relation between velocity and lift coefficient is evident here. The increment in lift with the positive change in velocity is observed at 15 degrees of angle of attack.

5.2 ANSYS WORKBENCH SIMULATIONS

After completing the wind tunnel experimentation, next simulations were carried out on ANSYS WORKBENCH. For ANSYS, firstly the geometry was imported from solid works and it was enclosed in a chamber, to replicate the wind tunnel scenario.

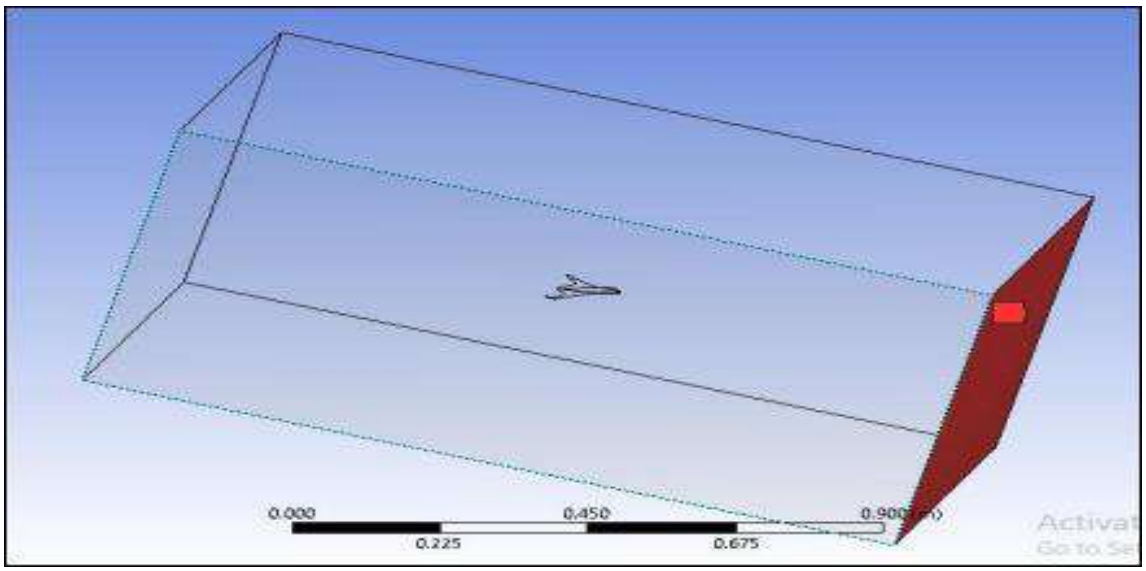

Figure 14: Wind tunnel chamber

Then for different angle of attack and wind velocities, the iterations were performed. Following are the results for those iterations:

5.2.1 FOR WIND VELOCITY 40 ms^{-1}

Following are the results of pressure contour at 40 ms^{-1} with 0-degree AOA. The pressure contours can be seen on the upper surface of the wing. The red region indicates the area of high pressure which is at the nose of the wing body. The highest pressure on the wing body is the nose tip of the BWB and the base of the wing. Lowest pressure can be seen on the wings leading edges indicated by blue region. The high pressure at the base and the low pressure at the top confirm that the wing is generating the force of lift.

The maximum pressure is $1.02x10^5$ Pascal and minimum pressure is at $1x10^5$ Pascal.

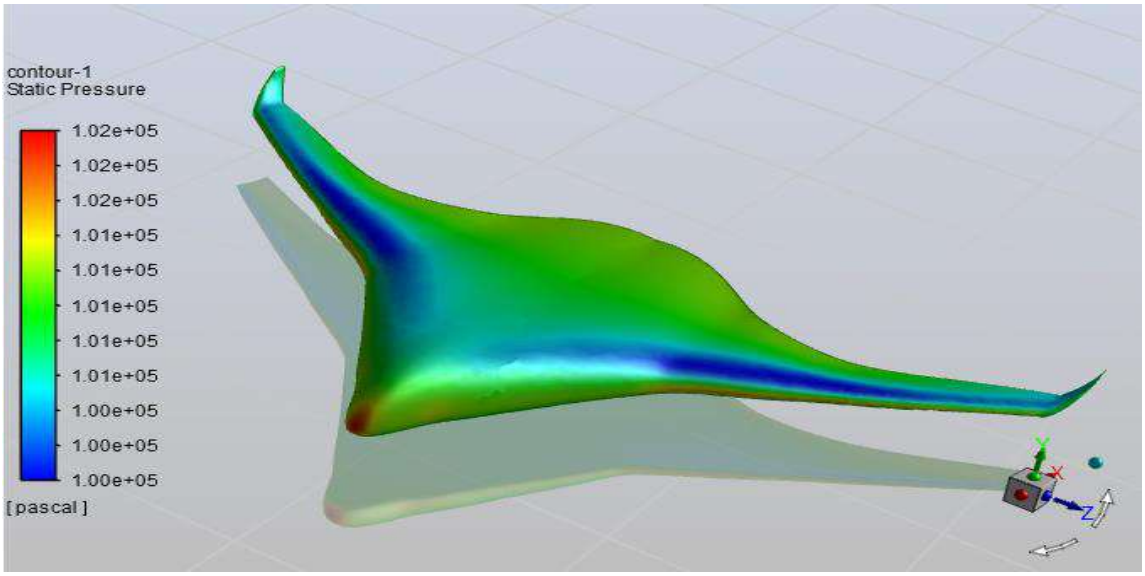

Figure 15: Static pressure for 0^0

The following graph is based on the number of iterations against coefficient of lift. The relation between CL and iterations is linear. The coefficient of lift increases with the number of iterations given to the system and becomes constant at the CL value of almost 0.008. This proves that the wing is generating lift at low speed at 40ms^{-1}.

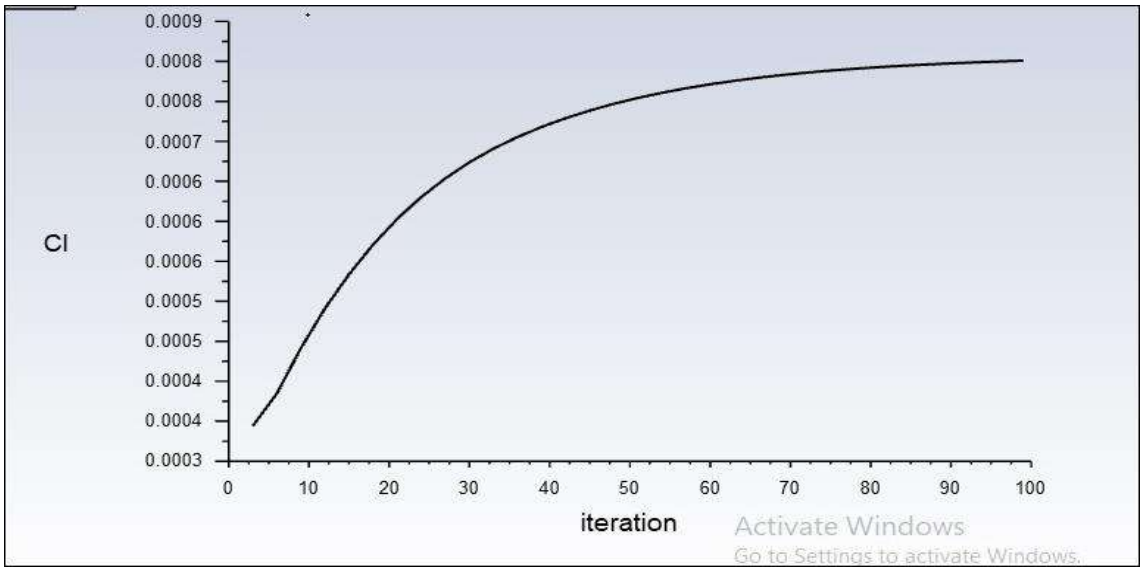

Figure 16: Coefficient of lift for 0^0

If we increase the AOA up to 5 degrees keeping the speed of air constant at $40ms^{-1}$ the behavior of the wing changes slightly which can be seen in the below image. The image shows the velocity vector of air at constant speed. The red vectors indicate high speed and the blue vectors indicate low speed. The green vectors show that the lift is generating. The lift can be seen increasing with the increase in angle of attack.

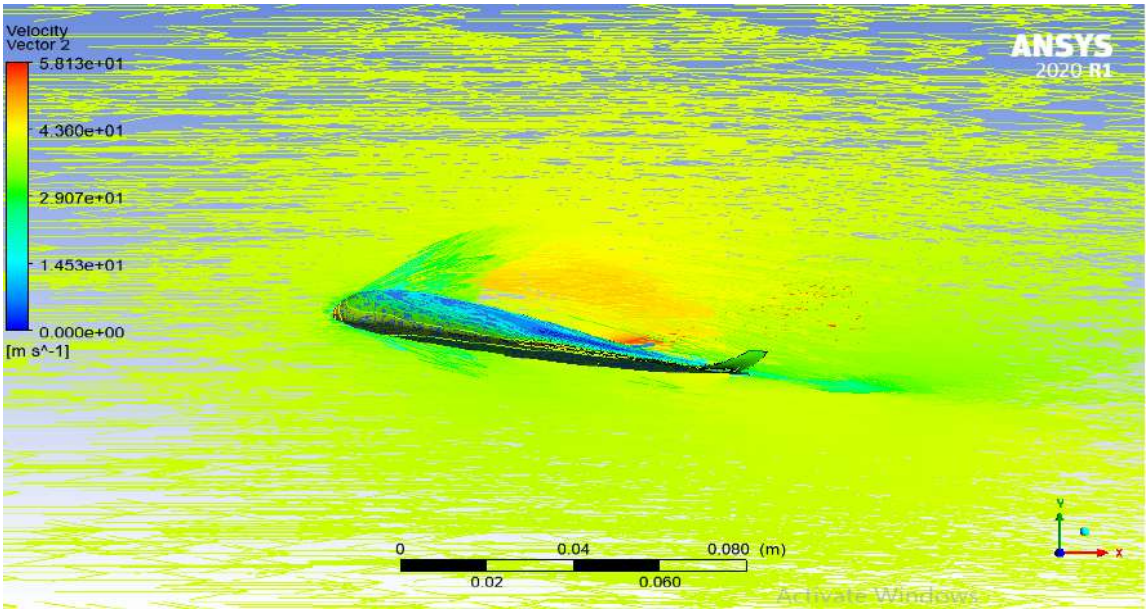

Figure 17: Velocity vector for 0^o

Similarly, with 40ms^{-1} at the 5 degrees AOA the lift can be seen increasing as the blue region on the wing is expanding. The high pressure at the base and at the nose pushes the plane up creating an up thrust and the low pressure region above the plane shows uplift in the blended wing.

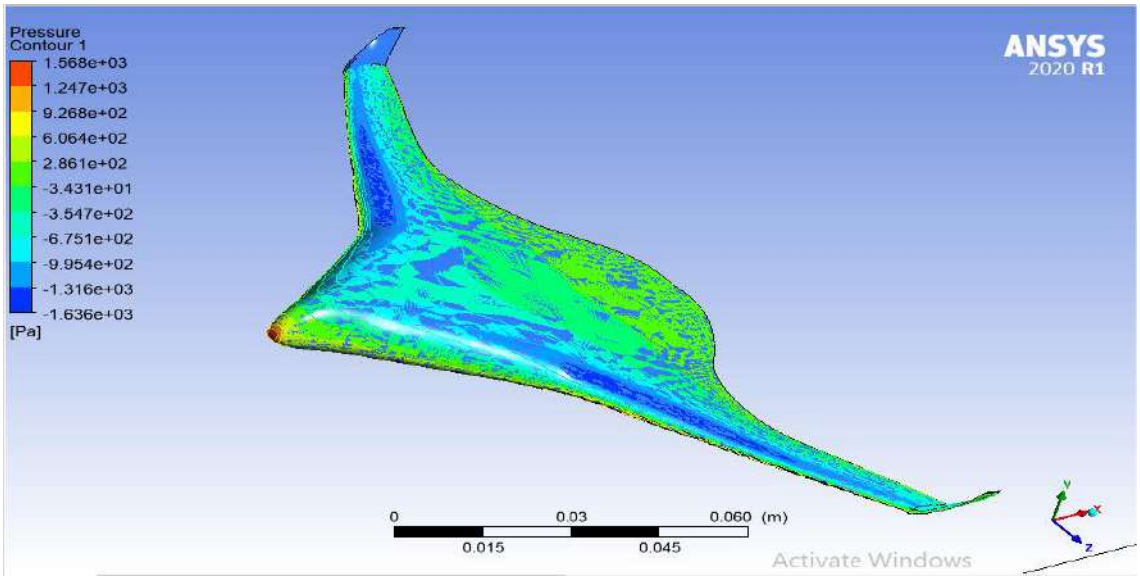

Figure 18: Pressure contour for 0^0

According to the graph of pressure magnitude and the number of iterations, the pressure with time is decreasing with the increase of iterations. It is an inverse relation and after 40 iterations the pressure became constant throughout the iterations.

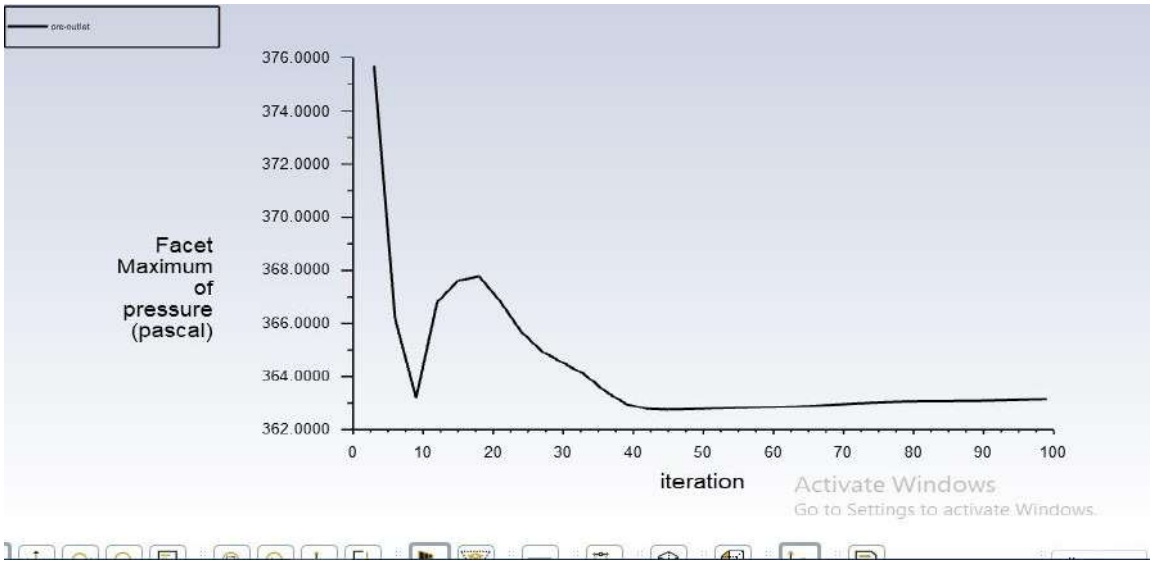

Figure 19: Pressure magnitude for 0^0

Following is the graph of velocity magnitude against the number of iterations. In the case of velocity magnitude graph with same conditions above the velocity is increasing with the increase in no of iterations accordingly. The velocity has reached its maximum value 40.01ms^{-1} and drastically decreased. It indicates that the system has stopped or the plane is not responding.

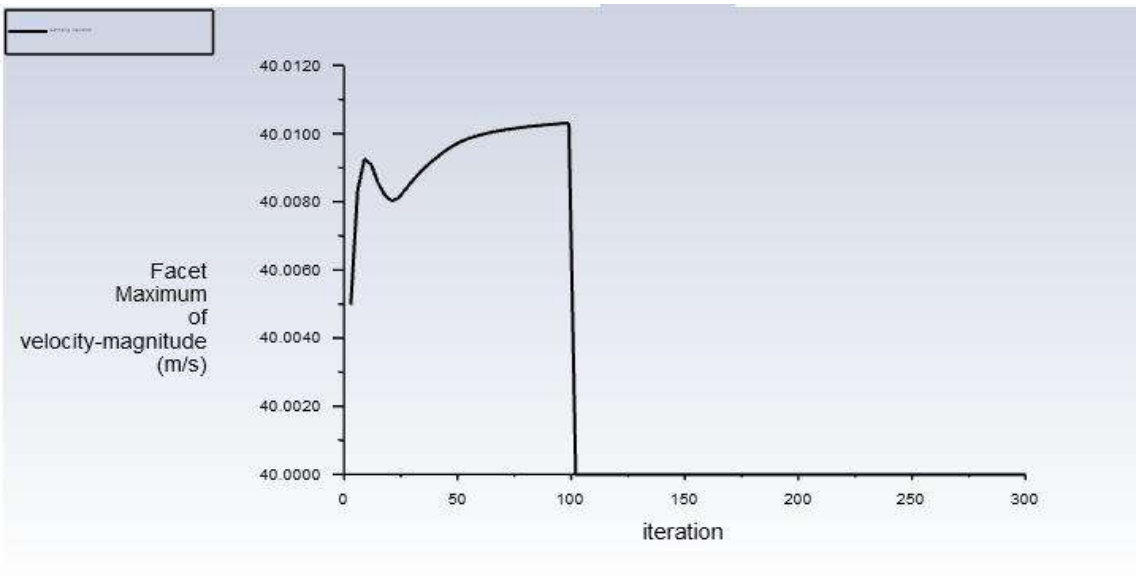

Figure 20: Velocity magnitude for 0^0

Now, we have taken the same speed and increased the AOA to 10 degrees in the wind tunnel with same conditions.

The low-pressure region can be seen increasing with the increase in angle of attack of wing. The pressure contour indicates the maximum value of at the nose tip and base which is approx. 1.588x10^3 Pascal and the low pressure the top of the wings is -1.63x10^3 Pascal. The lift is increasing with the increase in AOA but the pressure is going decreasing drastically on the top of the wing which is creating an up thrust on the wing even on low speed at 40m/s.

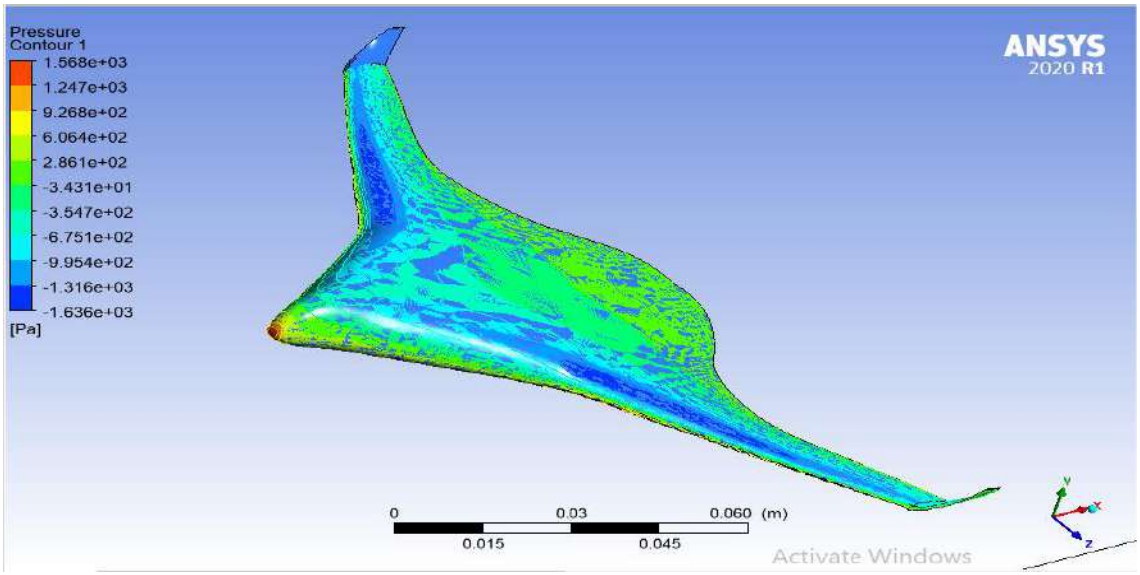

Figure 21: Pressure contour for 10^0

The Following image is velocity vector at 10 degrees AOA. The lift is generating when the velocity vectors are pushing the wing body upwards. At 10 degrees the maximum uplift of the vectors is 5.813x10 ms^{-1} and the low-speed vectors have the value of 1.45x10 ms^{-1}.

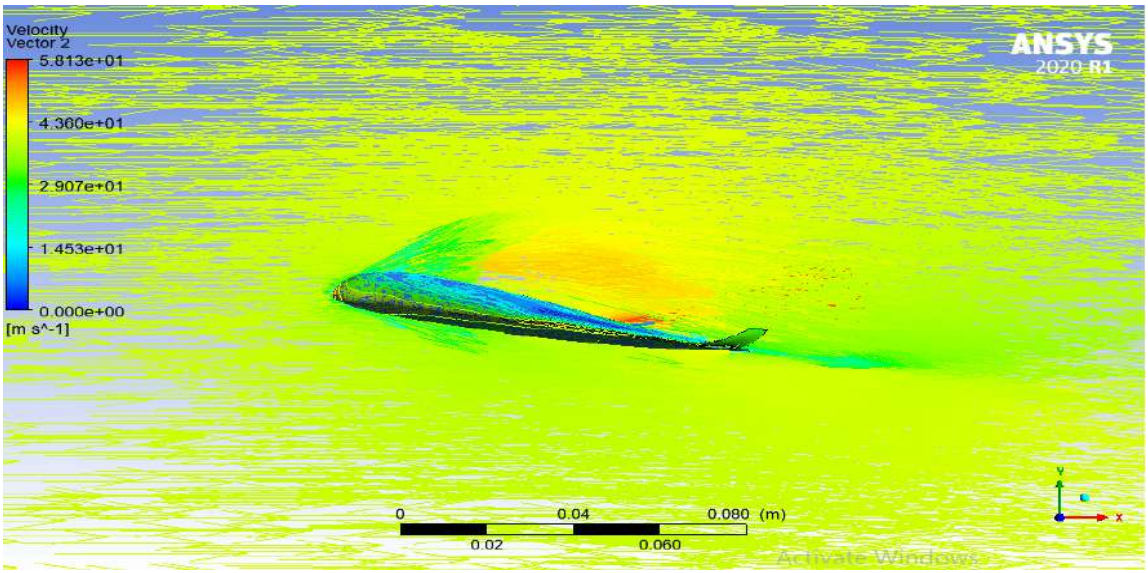

Figure 22: Velocity vector for 10^0

In the case of facet maximum pressure, the pressure is increasing up to maximum value of approx. 370 Pascal and after 10 iterations it stabilizes at the constant value of 370 Pascal.

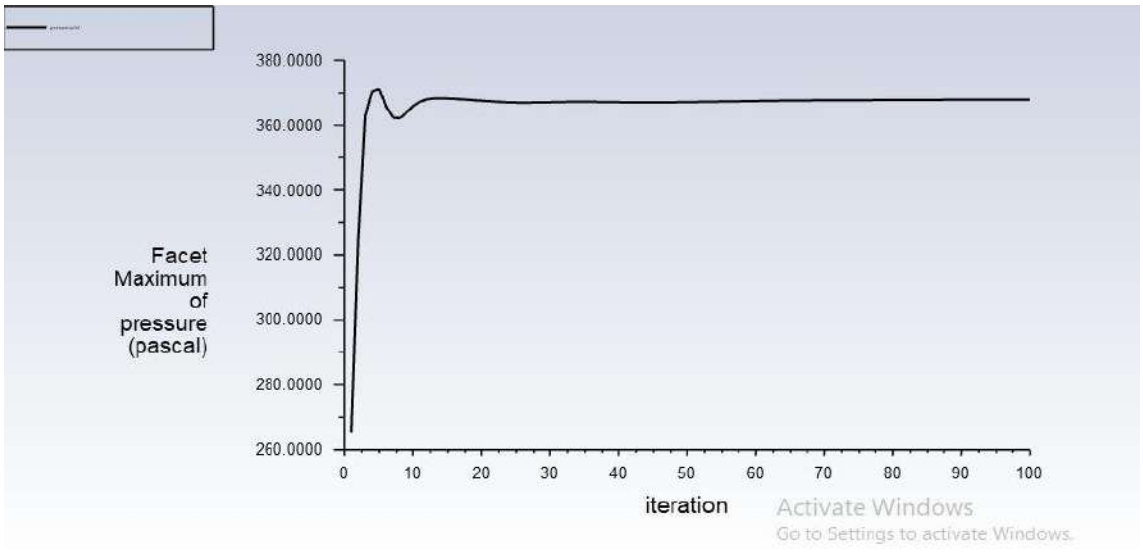

Figure 23: Pressure magnitude for 10^0

The coefficient of lift is increasing with the increase in number of iterations. The lift is increasing up to 0.0016 and after that it became constant. This result confirms that our simulations are correct and according to the required results.

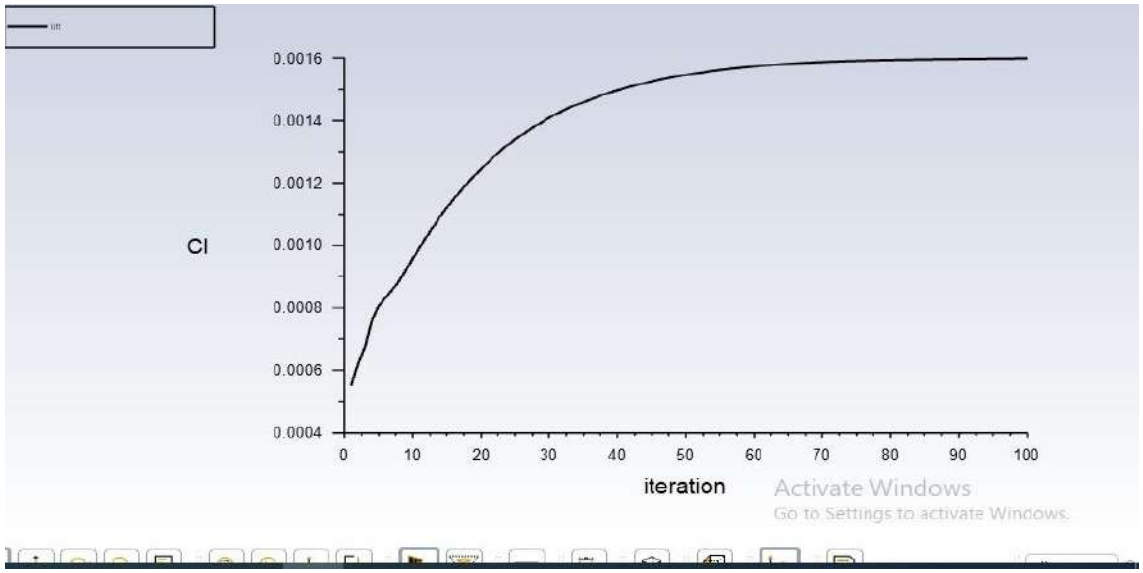

Figure 24: Coefficient of lift for 10^0

After this we have increased the AOA to 12 degrees keeping all variable constant. The wind velocity is at $40ms^{-1}$. This image is from the front of the plane from where we can see the

maximum stresses and pressure at the nose of the plane and the leading edges of the whole aero foil. The maximum pressure is $1.56x10^3$ Pascal and low pressure region is at $-1.810x10^3$ Pascal.

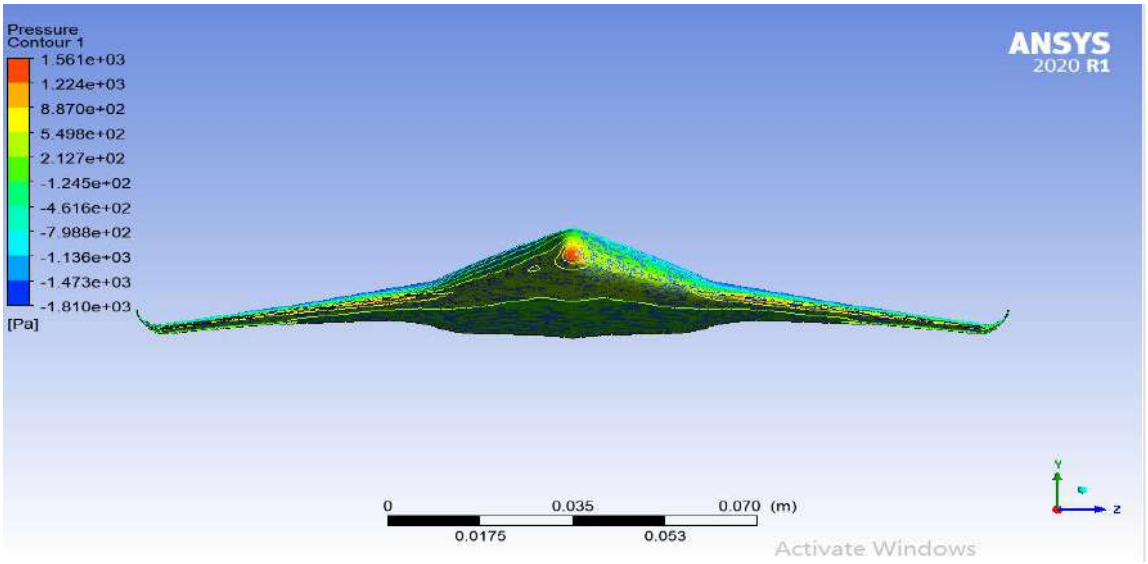

Figure 25: Pressure contour for 12^0

The following image is the same pressure contour simulation but from the bottom view. We can see the pressure with increase in angle of attack above 10 degrees is also decreasing the bottom edge indicates mostly green region which is moderate pressure. The lift is decreasing when the AOA is increasing above 10 degrees but still gives a positive value at low speed.

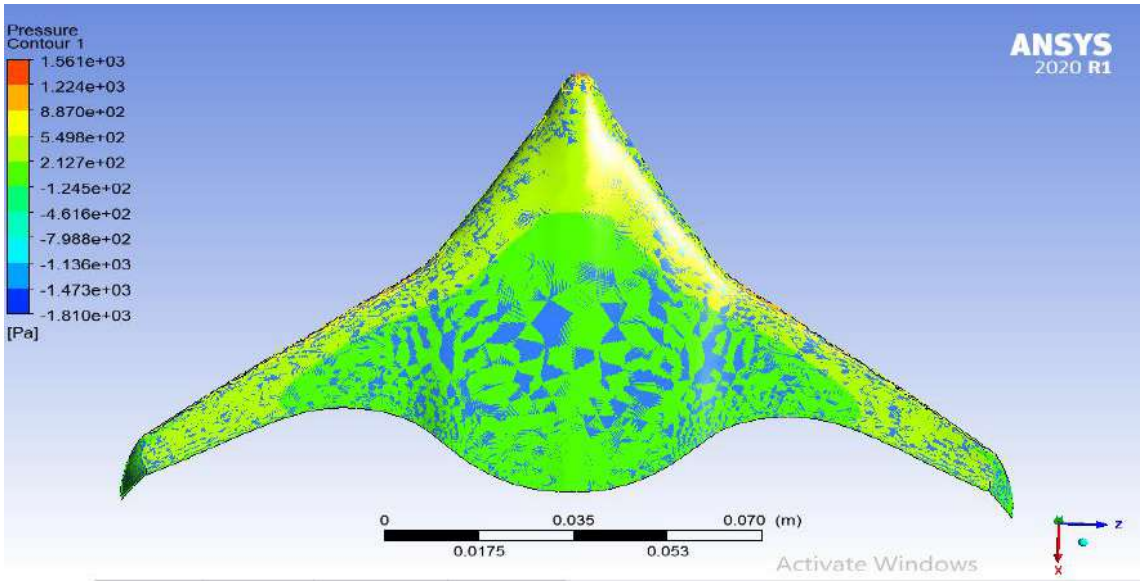

Figure 26: Pressure contour for 12^0

Similarly, the pressure contour at an isometric view to analyze the behavior of the plane more thoroughly. We have observed that the low-pressure region above the plane is increasing as well as there is decrease in pressure at the rear end of the plane.

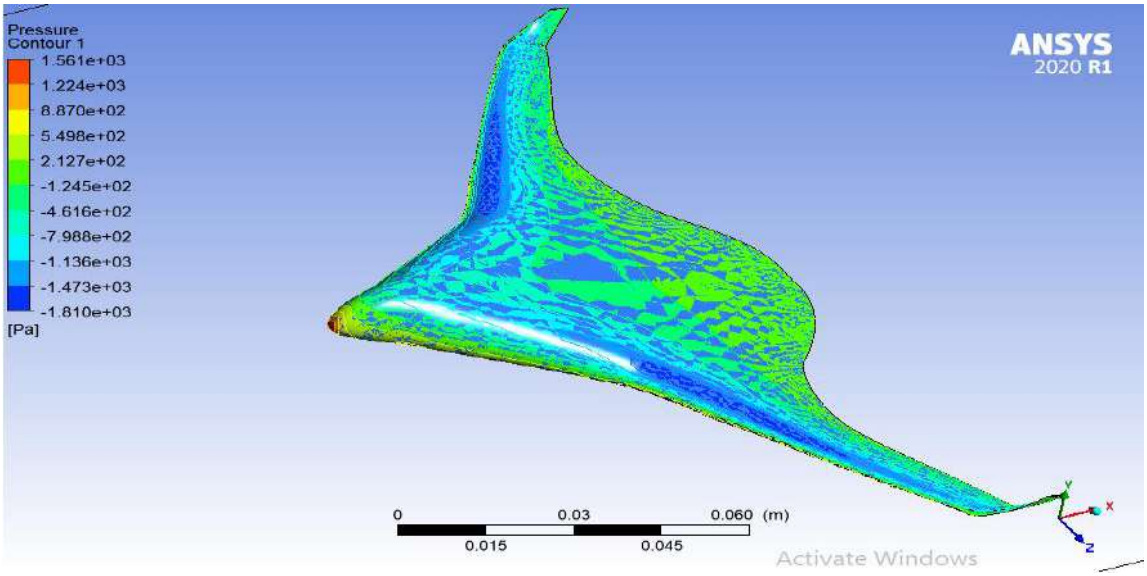

Figure 27: Pressure contour for 12^0

The facet maximum of velocity magnitude is also increasing with the number of iterations like the previous readings. The following graphs show that the velocity is increasing gradually with the increase in number of iterative values. It is a linear response which indicates that our simulations are running smoothly.

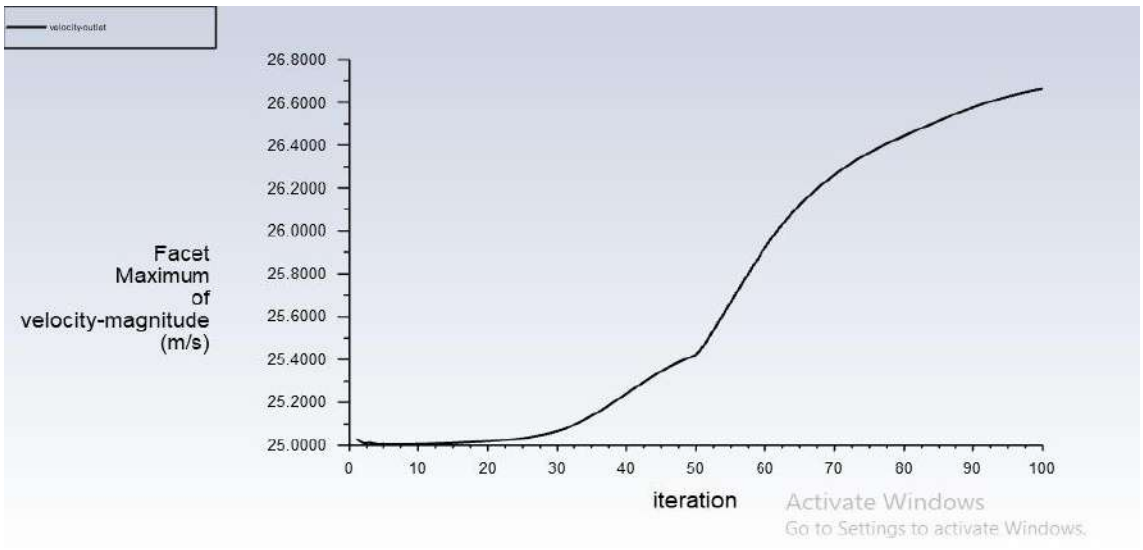

Figure 28: Velocity magnitude for 12^0

5.2.2. FOR WIND VELOCITY 30 MS^{-1}

After the simulations performed on 40ms^{-1} wind velocity, we decreased it to 30ms^{-1} and performed similarly with different angle of attack to validate and observe the behavior of low speed on lift. We also observed the change in lift with variable AOA at velocity 30ms^{-1}.

In diagram the plane axis is in coincident with x-axis. The AOA is 0 degrees, and the speed is constant. We have a pressure contour in which we can observe the maximum pressure at $1.02x10^5$ Pascal and low pressure $1.00x10^5$ Pascal at the wings leading edges which are indicated by blue region.

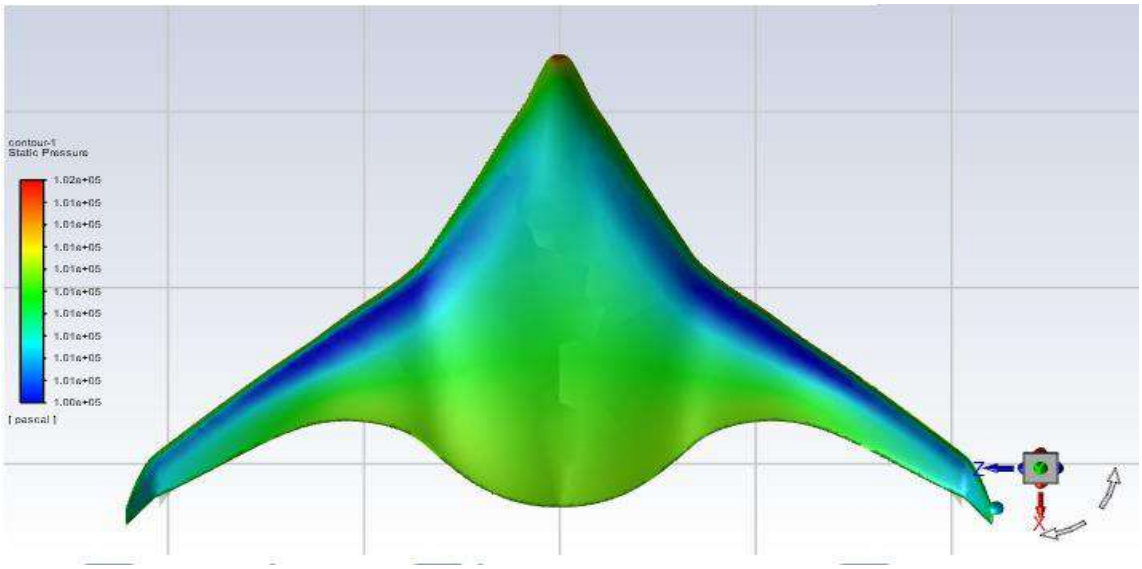

Figure 29: Static pressure at 0^0 (a)

The figure shows the static pressure of the plane at 0 degrees angle of attack in an isometric view. The red region of high pressure can be seen more clearly in this view. The maximum and minimum pressures are discussed in above figure description. The lift at 0 degrees and 30ms^{-1} is lower than at 40ms^{-1}.

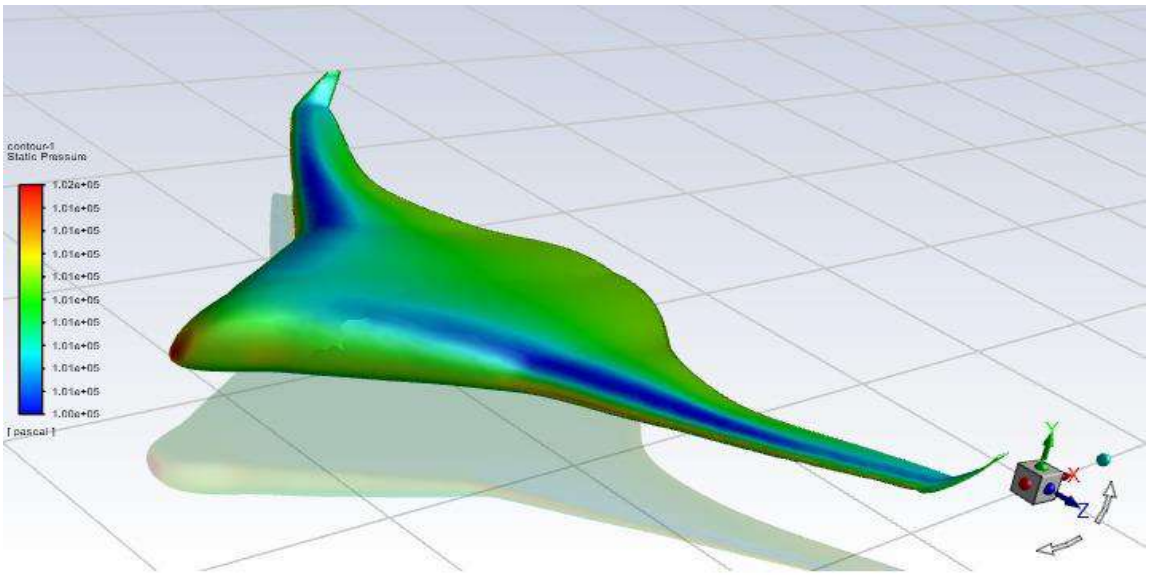

Figure 30: Static pressure 0^0 (b)

This figure is a graph of coefficient of lift and number of iterations. As discussed above the lift generated is less than the lift generated when the initial conditions were with velocity $40ms^{-1}$. This is because the lower the speed the up thrust required for a lift will decrease. The value of CL is increased rapidly and then decreased but after 20 iterations it became constant.

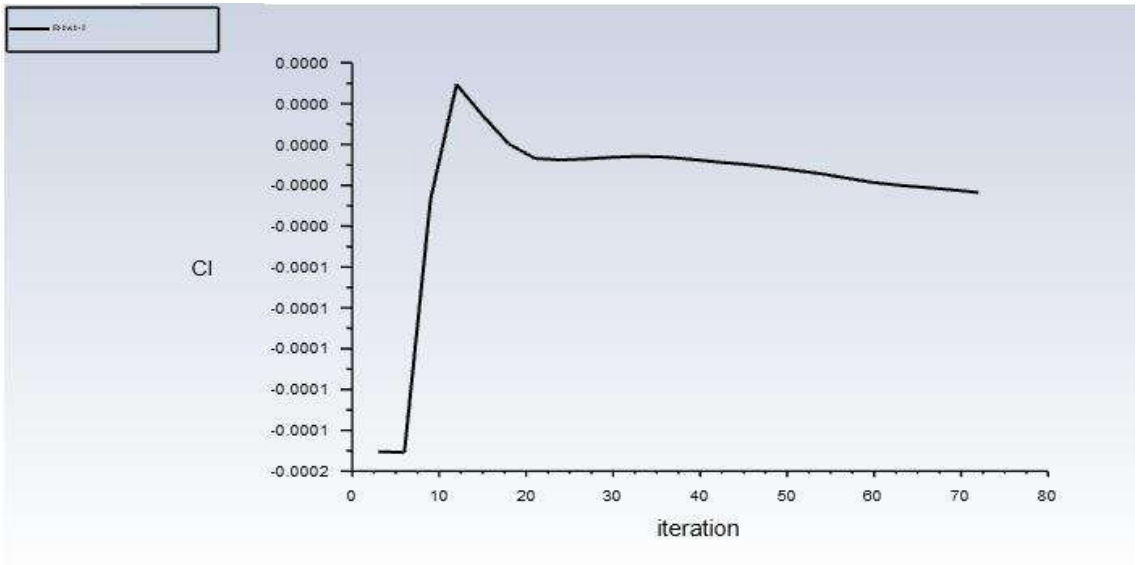

Figure 31: Coefficient of lift for 0^0

For the maximum pressure, the figure gives us a graph between pressure and number of iterations for simulations. The pressure is decreasing with the increase in number of iterations

and becomes stable. When the simulation of plane starts, the pressure is highest and after almost 15 iterations it has stabilized itself with the increase in iterations. The pressure becomes constant at value of almost 101530 Pascal which is slightly higher than the atmospheric pressure.

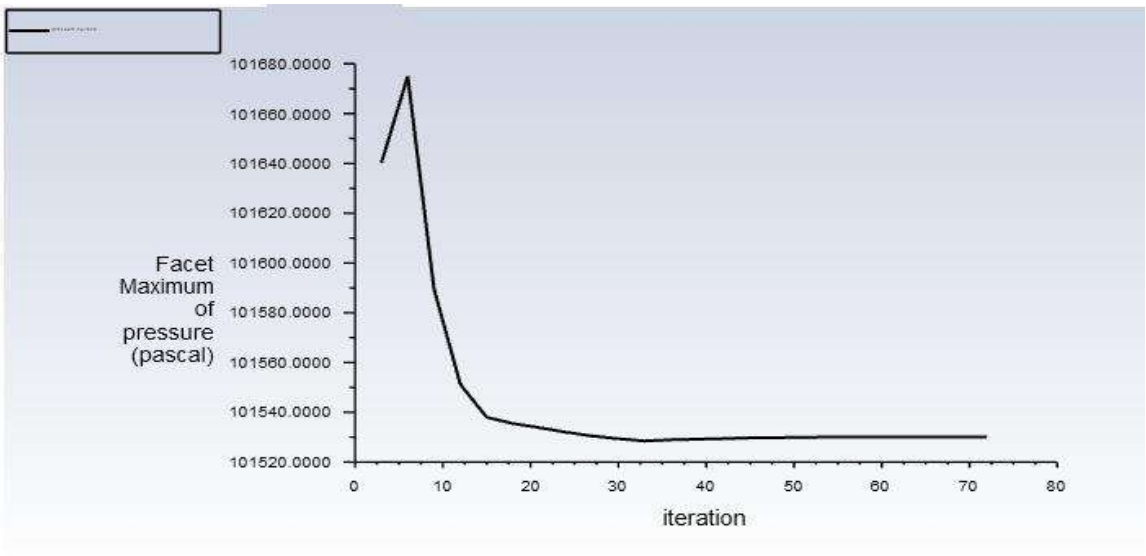

Figure 32: Pressure magnitude

Similarly, we have run the same analysis with same initial conditions and the approximations of pressure values were a little different but followed the same trend. The figure has the pressure value which stabilizes itself at pressure 101510 Pascal but this time it stabilized itself after 110 iterations.

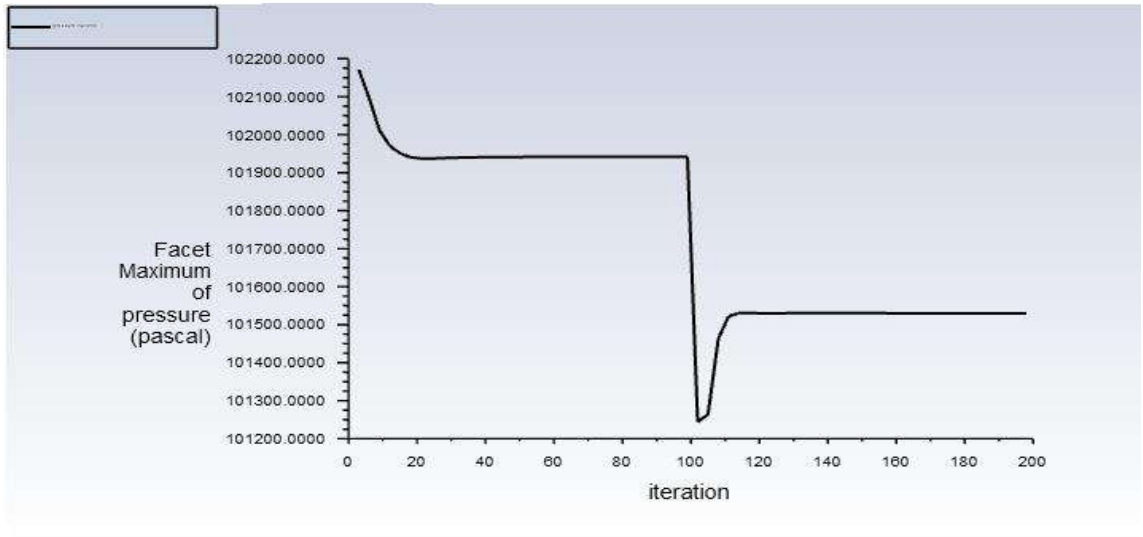

Figure 33: Maximum Pressure regions (a)

After the third attempt of running the same analysis under same initial conditions we observed the same trend of decreasing pressure and stabilization of pressure. As, the figure indicates, the pressure is decreased from 102200 Pascal to 101250 Pascal which is close to atmospheric pressure after almost 200 iterations. The facet maximum of pressure has achieved constant value.

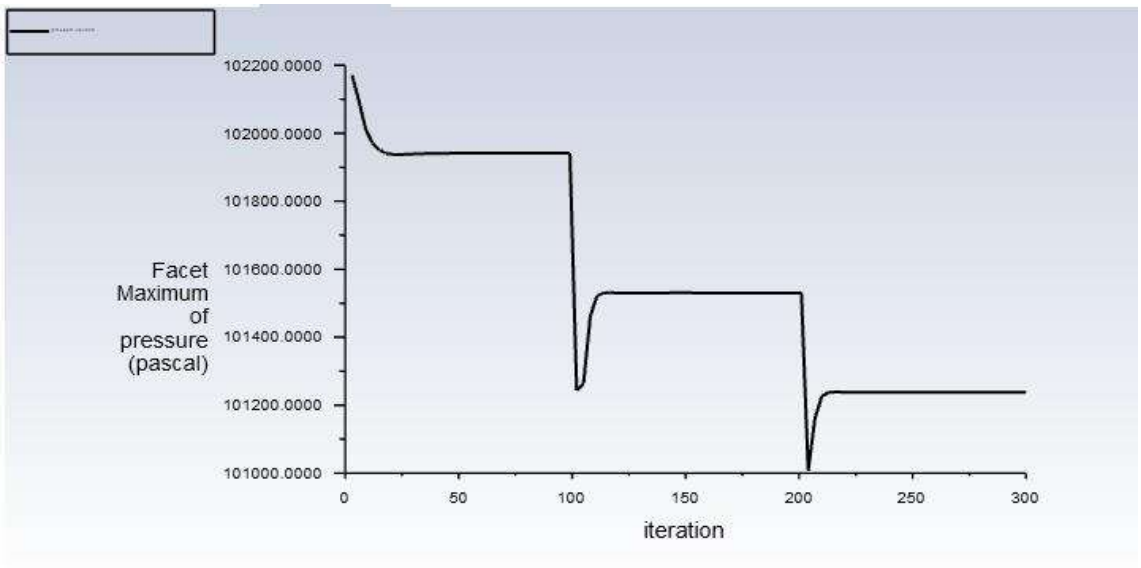

Figure 34: Maximum pressure regions (b)

The velocity magnitude graph in figure mimics the real time data where the velocity is increasing with time and number of iterations. We can see a linear trend in which the velocity is gradually increasing from $0ms^{-1}$ to $25.25ms^{-1}$ and going above up to $30ms^{-1}$ which was given in the initial conditions. This trend shows that there is 15% error which can be neglected as these are only assumptions.

5.3 CONCULSION

The project was to analyze the aerodynamic parameters for aircraft, basically a blended wing body, with self-selected aero foils for low speed analysis. The primary aim of selection of aero foil MH78 was due to its spherical leading edge which helps preventing stalling behavior at low speed but high angle of attack. The second aero foil, S1223 is one of the most preferred aero foils for low speed crafts. For a craft to remain in air, it needs to generate constant lift to prevent an undesired event or performance. At low speed, as the angle of attack is gradually given an

increment, the chances of stalling become equal to certainty but of reduction in lift generation and usually the conventional plane stalls at 12 degrees. But this craft gave its positive lift value till 15 degrees which makes it one of the most optimized designs overall and correspondingly making its efficient one. At 12 degrees, positive lift value still remains and the craft continued its flight. The error between the wind tunnel experimentation and ANSYS simulation existed between 10 to 15 percent due to difference in ideal and actual conditions. Its 3D printed model was tested in wind tunnel and scaled up models free flight testing was done in open air. Both of them showed a positive behavior till 15 degrees of angle of attack but low speed. Hence, this brand new prototype is an excellent low speed aircraft design.

CHAPTER 6

REFERENCES

[1] A. Vavalle, "Aerodynamic considerations of blended wing body aircraft", [Online]. Available: https://www.sciencedirect.com/science/article/pii/S0376042104000569?via%3Dihub

[2] N. Qin, A. Vavalle, A. Le Moigne, M. Laban, K. Hackett, and P. Weinerfelt, "Aerodynamic considerations of blended wing body aircraft," *Prog. Aerosp. Sci.*, vol. 40, no. 6, pp. 321–343, Aug. 2004, doi: 10.1016/j.paerosci.2004.08.001.

[3] R. T. Britt, S. B. Jacobson, and T. D. Arthurs, "Aeroservoelastic Analysis of the B-2 Bomber," *J. Aircr.*, vol. 37, no. 5, pp. 745–752, Sep. 2000, doi: 10.2514/2.2674.

[4] B. R.t and V. J.A, "Aeroservoelastic Characteristics of the B-2 Bomber and Implications for Future Large Aircraft," p. 12, May 2000.

[5] R. Liebeck, M. Page, and B. Rawdon, "Blended-wing-body subsonic commercial transport," in *36th AIAA Aerospace Sciences Meeting and Exhibit*, Reno,NV,U.S.A.: American Institute of Aeronautics and Astronautics, Jan. 1998. doi: 10.2514/6.1998-438.

[6] K. A. Deere, J. M. Luckring, S. N. McMillin, J. D. Flamm, and D. Roman, "CFD Predictions for Transonic Performance of the ERA Hybrid Wing-Body Configuration (Invited)," in *54th AIAA Aerospace Sciences Meeting*, San Diego, California, USA: American Institute of Aeronautics and Astronautics, Jan. 2016. doi: 10.2514/6.2016-0266.

[7] "UNICEF and the Sustainable Development Goals".

[8] H. J. Shim and S. O. Park, "Low-speed Wind-tunnel Test Results of a BWB-UCAV Model," *Procedia Eng.*, vol. 67, pp. 50–58, 2013, doi: 10.1016/j.proeng.2013.12.004.

[9] P. Dehpanah and A. Nejat, "The aerodynamic design evaluation of a blended-wing-body configuration," *Aerosp. Sci. Technol.*, vol. 43, pp. 96–110, Jun. 2015, doi: 10.1016/j.ast.2015.02.015.

[10] L. Wang, N. Zhang, H. Liu, and T. Yue, "Stability characteristics and airworthiness requirements of blended wing body aircraft with podded engines," *Chin. J. Aeronaut.*, vol. 35, no. 6, pp. 77–86, Jun. 2022, doi: 10.1016/j.cja.2021.09.002.

[11] A. Suresh and S. Rajakumar, “Design of small horizontal axis wind turbine for low wind speed rural applications,” *Mater. Today Proc.*, vol. 23, pp. 16–22, 2020, doi: 10.1016/j.matpr.2019.06.008.

[12] R. E. M. Nasir, W. Kuntjoro, and W. Wisnoe, “Aerodynamic, Stability and Flying Quality Evaluation on a Small Blended Wing-body Aircraft with Canard Foreplanes,” *Procedia Technol.*, vol. 15, pp. 783–791, 2014, doi: 10.1016/j.protcy.2014.09.051.

[13] R. H. Liebeck, “Design of the Blended Wing Body Subsonic Transport,” *J. Aircr.*, vol. 41, no. 1, pp. 10–25, Jan. 2004, doi: 10.2514/1.9084.

[14] A. Valiyff and M. Arjomandi, “An Investigation Into the Aerodynamic Efficiency of Tailles Aircraft,” in *47th AIAA Aerospace Sciences Meeting including The New Horizons Forum and Aerospace Exposition*, Orlando, Florida: American Institute of Aeronautics and Astronautics, Jan. 2009. doi: 10.2514/6.2009-1436.

[15] P. Li, B. Zhang, Y. Chen, C. Yuan, and Y. Lin, “Aerodynamic Design Methodology for Blended Wing Body Transport,” *Chin. J. Aeronaut.*, vol. 25, no. 4, pp. 508–516, Aug. 2012, doi: 10.1016/S1000-9361(11)60414-7.

[16] G. Yu and Y. Duan, “Design Improvement of a BWB Aerodynamic Performance at Cruise and Take-Off Speeds,” *Int. J. Aerosp. Eng.*, vol. 2022, pp. 1–18, Nov. 2022, doi: 10.1155/2022/5216387.

[17] M. Brown and R. Vos, “Conceptual Design and Evaluation of Blended-Wing Body Aircraft,” in *2018 AIAA Aerospace Sciences Meeting*, Kissimmee, Florida: American Institute of Aeronautics and Astronautics, Jan. 2018. doi: 10.2514/6.2018-0522.

[18] M. Bishara, P. Horst, H. Madhusoodanan, M. Brod, B. Daum, and R. Rolfes, “A Structural Design Concept for a Multi-Shell Blended Wing Body with Laminar Flow Control,” *Energies*, vol. 11, no. 2, p. 383, Feb. 2018, doi: 10.3390/en11020383.

[19] T. Mulyanto and M. L. Nurhakim, “CONCEPTUAL DESIGN OF BLENDED WING BODY BUSINESS JET AIRCRAFT,” *J. KONES Powertrain Transp.*, vol. 20, no. 4, pp. 299–306, Jan. 2015, doi: 10.5604/12314005.1137630.

[20] Z. Lyu and J. R. R. A. Martins, “Aerodynamic Design Optimization Studies of a Blended-Wing-Body Aircraft,” *J. Aircr.*, vol. 51, no. 5, pp. 1604–1617, Sep. 2014, doi: 10.2514/1.C032491.

[21] K. Lehmkuehler and K. Wong, “DESIGN AND TEST OF A UAV BLENDED WING BODY CONFIGURATION,” p. 11.

[22] R. Vos, F. J. J. M. M. Geuskens, and M. F. M. Hoogreef, “A New Structural Design Concept for Blended Wing Body Cabins,” in *53rd AIAA/ASME/ASCE/AHS/ASC Structures, Structural Dynamics and Materials Conference
20th AIAA/ASME/AHS Adaptive Structures Conference
14th AIAA*, Honolulu, Hawaii: American Institute of Aeronautics and Astronautics, Apr. 2012. doi: 10.2514/6.2012-1998.

[23] O. HARRISSON, “Aerodynamic Analysis of a Blended Wing Body UAV,” p. 18.

[24] M. Alessandro and Porcarelli, “Development of a CFD model and methodology for the internal flow simulation in a hydrogen-powered UAV,” 2021.

[25] L. U. Hansen, W. Heinze, and P. Horst, “Blended wing body structures in multidisciplinary pre-design,” *Struct. Multidiscip. Optim.*, vol. 36, no. 1, pp. 93–106, Jul. 2008, doi: 10.1007/s00158-007-0161-z.

[26] L. Ayuso Moreno and R. Sant Palma, “AERODYNAMIC STUDY OF A BLENDED WING BODY; COMPARISON WITH A CONVENTIONAL TRANSPORT AIRPLANE,” p. 8.

[27] D. Howe, “Blended wing body airframe mass prediction,” *Proc. Inst. Mech. Eng. Part G J. Aerosp. Eng.*, vol. 215, no. 6, pp. 319–331, Jun. 2001, doi: 10.1243/0954410011533329.

[28] R. Ma, B. Zhong, and P. Liu, “MULTI-OBJECTIVE OPTIMIZATION DESIGN OF LOWREYNOLDS-NUMBER AIRFOILS S1223,” p. 10.

[29] R. Ma and P. Liu, “Numerical Simulation of Low-Reynolds-Number and High-Lift Airfoil S1223,” p. 6.

[30] M. Voskuijl, and G. La Rocca, “CONTROLLABILITY OF BLENDED WING BODY AIRCRAFT,” p. 10.

[31] A. MEYER STRÖBORG, “Aerodynamic Analysis of Reflex Airfoils at Low Reynolds Numbers,” p. 28.

[32] A. A. Alsahlani, “A Study of Impacts of Airfoil Geometry on the Aerodynamic Performance at Low Reynolds Number,” *Int. J. Mech. Eng. Robot. Res.*, pp. 99–106, 2023, doi: 10.18178/ijmerr.12.2.99-106.

[33] A. A. Alsahlani, “A Study of Impacts of Airfoil Geometry on the Aerodynamic Performance at Low Reynolds Number,” *Int. J. Mech. Eng. Robot. Res.*, pp. 99–106, 2023, doi: 10.18178/ijmerr.12.2.99-106.

[34] D. Vicroy, “Blended-Wing-Body Low-Speed Flight Dynamics: Summary of Ground Tests and Sample Results (Invited),” in *47th AIAA Aerospace Sciences Meeting including The New Horizons Forum and Aerospace Exposition*, Orlando, Florida: American Institute of Aeronautics and Astronautics, Jan. 2009. doi: 10.2514/6.2009-933.

[35] R. Liebeck, M. Page, and B. Rawdon, “Blended-wing-body subsonic commercial transport,” in *36th AIAA Aerospace Sciences Meeting and Exhibit*, Reno,NV,U.S.A.: American Institute of Aeronautics and Astronautics, Jan. 1998. doi: 10.2514/6.1998-438.

[36] D. Thompson, J. Feys, M. Filewich, S. Abdel-Magid, D. Dalli, and F. Goto, “The Design and Construction of a Blended Wing Body UAV,” in *49th AIAA Aerospace Sciences Meeting including the New Horizons Forum and Aerospace Exposition*, Orlando, Florida: American Institute of Aeronautics and Astronautics, Jan. 2011. doi: 10.2514/6.2011-841.

[37] Z. Lyu and J. R. R. A. Martins, “Aerodynamic Design Optimization Studies of a Blended-Wing-Body Aircraft,” *J. Aircr.*, vol. 51, no. 5, pp. 1604–1617, Sep. 2014, doi: 10.2514/1.C032491.

[38] I. H. ABBOTT, *THEORY OF WING SECTIONS*.

[39] M. Bauer, T. Grund, W. Nitsche, and V. Ciobaca, “Wing Tip Drag Reduction at Nominal Take-Off Mach Number: An Approach to Local Active Flow Control with a Highly Robust Actuator System,” *Aerospace*, vol. 3, no. 4, p. 36, Oct. 2016, doi: 10.3390/aerospace3040036.

[40] E. Ordoukhanian and A. M. Madni, “Blended Wing Body Architecting and Design: Current Status and Future Prospects,” *Procedia Comput. Sci.*, vol. 28, pp. 619–625, 2014, doi: 10.1016/j.procs.2014.03.075.

[41] Y. Zhang, W. J. Sung, and D. N. Mavris, “Application of Convolutional Neural Network to Predict Airfoil Lift Coefficient,” in *2018 AIAA/ASCE/AHS/ASC Structures, Structural Dynamics, and Materials Conference*, Kissimmee, Florida: American Institute of Aeronautics and Astronautics, Jan. 2018. doi: 10.2514/6.2018-1903.

[42] R. J. Adrian, “Particle-Imaging Techniques for Experimental Fluid Mechanics,” *Annu. Rev. Fluid Mech.*, vol. 23, no. 1, pp. 261–304, Jan. 1991, doi: 10.1146/annurev.fl.23.010191.001401.

[43] M. Reid and J. Kozak, “Thin/Cambered/Reflexed Airfoil Development for Micro Air Vehicle Applications at Reynolds Numbers of 60,000 to 100,000,” in *AIAA Atmospheric Flight Mechanics Conference and Exhibit*, Keystone, Colorado: American Institute of Aeronautics and Astronautics, Aug. 2006. doi: 10.2514/6.2006-6832.

[44] I. N. Wani *et al.*, “Design & analysis of NACA 0012 airfoil with circular dent of 30 mm depth on upper surface,” *Mater. Today Proc.*, p. S2214785323026342, May 2023, doi: 10.1016/j.matpr.2023.05.013.

[45] Hidayatullah Mohammad Ali, Azmin Shakrine Mohd Rafie, and Syaril Azrad Md Ali, “Numerical Analysis of Leading Edge Cylinder Aerofoil on Selig S1223 for Moving Surface Boundary Control,” *J. Aeronaut. Astronaut. Aviat.*, vol. 53, no. 2, Jun. 2021, doi: 10.6125/JoAAA.202106_53(2).06.

[46] D. Raymer, *Aircraft Design: A Conceptual Approach, Fifth Edition*. Washington, DC: American Institute of Aeronautics and Astronautics, Inc., 2012. doi: 10.2514/4.869112.

[47] W. F. Phillips, “Lifting-Line Analysis for Twisted Wings and Washout-Optimized Wings,” *J. Aircr.*, vol. 41, no. 1, pp. 128–136, Jan. 2004, doi: 10.2514/1.262.

[48] D. Liu, B. Song, W. Yang, X. Yang, D. Xue, and X. Lang, “A Brief Review on Aerodynamic Performance of Wingtip Slots and Research Prospect,” *J. Bionic Eng.*, vol. 18, no. 6, pp. 1255–1279, Nov. 2021, doi: 10.1007/s42235-021-00116-6.

[49] J. Johansen and N. N. Sørensen, “Aerofoil characteristics from 3D CFD rotor computations,” *Wind Energy*, vol. 7, no. 4, pp. 283–294, Oct. 2004, doi: 10.1002/we.127.

[50] J. Warham, “Wing loadings, wing shapes, and flight capabilities of procellariiformes,” *N. Z. J. Zool.*, vol. 4, no. 1, pp. 73–83, Mar. 1977, doi: 10.1080/03014223.1977.9517938.

[51] P. Bauer, R. Venkataraman, B. Vanek, P. J. Seiler, and J. Bokor, “Fault Detection and Basic In-Flight Reconfiguration of a Small UAV Equipped with Elevons,” *IFAC-Pap.*, vol. 51, no. 24, pp. 600–607, 2018, doi: 10.1016/j.ifacol.2018.09.637.

[52] R. Cavallaro and L. Demasi, “Challenges, Ideas, and Innovations of Joined-Wing Configurations: A Concept from the Past, an Opportunity for the Future,” *Prog. Aerosp. Sci.*, vol. 87, pp. 1–93, Nov. 2016, doi: 10.1016/j.paerosci.2016.07.002.

[53] W. F. Phillips, “Lifting-Line Analysis for Twisted Wings and Washout-Optimized Wings,” *J. Aircr.*, vol. 41, no. 1, pp. 128–136, Jan. 2004, doi: 10.2514/1.262.

[54] M. Smith, N. Komerath, R. Ames, O. Wong, and J. Pearson, “Performance analysis of a wing with multiple winglets,” in *19th AIAA Applied Aerodynamics Conference*, Anaheim,CA,U.S.A.: American Institute of Aeronautics and Astronautics, Jun. 2001. doi: 10.2514/6.2001-2407.

[55] M. D. Maughmer, “Design of Winglets for High-Performance Sailplanes,” *J. Aircr.*, vol. 40, no. 6, pp. 1099–1106, Nov. 2003, doi: 10.2514/2.7220.